

Tectonics

RESEARCH ARTICLE

10.1029/2018TC005119

Key Points:

- U–Pb detrital zircon ages and paleocurrent measurements from the Campanian–Maastrichtian turbidites of the central Pontides, Turkey
- A drastic change in the provenance of the Cretaceous turbidites of the central Pontides triggered by the opening of the Black Sea
- Prerift sandstone were sourced by the Ukrainian Shield; postrift sandstones were mostly sourced by the coeval Pontide magmatic arc

Supporting Information:

- Supporting Information S1
- Data Set S1

Correspondence to:

R. Akdoğan,
remziyeak@gmail.com

Citation:



Akdoğan, R., Okay, A. I., & Dunkl, I. (2019). Striking variation in the provenance of the Lower and Upper Cretaceous turbidites in the central Pontides (northern Turkey) related to the opening of the Black Sea. *Tectonics*, 38. <https://doi.org/10.1029/2018TC005119>

Received 21 APR 2018

Accepted 19 FEB 2019

Accepted article online 20 FEB 2019

Striking Variation in the Provenance of the Lower and Upper Cretaceous Turbidites in the Central Pontides (Northern Turkey) Related to the Opening of the Black Sea

R. Akdoğan^{1,2,3} , A. I. Okay^{1,4} , and I. Dunkl²
¹Faculty of Mines, Department of Geology, Istanbul Technical University, Maslak, Turkey, ²Geoscience Centre, Sedimentology and Environmental Geology, University of Göttingen, Göttingen, Germany, ³Now at State Key Laboratory of Mineral Deposits Research, School of Earth Sciences and Engineering, Nanjing University, Nanjing, China, ⁴Istanbul Technical University, Eurasia Institute of Earth Sciences, Maslak, Turkey

Abstract The Lower and Upper Cretaceous turbidites cover large areas in the central Pontides (north-central Turkey). The Lower Cretaceous turbidites are over 2 km thick and are exposed in an area of 400 × 90 km. The Upper Cretaceous (Campanian–Maastrichtian) forearc turbidites are up to 1,200 m thick and crop out in NW–SE trending elongate basins about 40 km wide, extending along the central and eastern Pontides. We present new detrital zircon U–Pb ages, petrography, and paleocurrent measurements from the Campanian–Maastrichtian turbidites and compare them to those from the Lower Cretaceous turbidites. The Campanian–Maastrichtian sandstones are dominated by carbonate and magmatic lithic grains. The paleocurrents indicate paleoflow directions parallel to the axis of the basin. The sandstones are dominated by Late Cretaceous zircons indicating derivation mainly from the coeval magmatic arc. In contrast, the Lower Cretaceous sandstones are dominated by quartz and feldspar, and paleocurrents indicate southward transport. The detrital zircons in the Lower Cretaceous sandstones are mainly Archean and Paleoproterozoic, indicating that in the Early Cretaceous, the source of turbidites was from the Archean–Paleoproterozoic Ukrainian Shield to the north. After the opening of the Black Sea in the Late Cretaceous, the connection between the Pontides and the East European Platform was severed and the Campanian–Maastrichtian turbidites were sourced principally from the magmatic arc in the Pontides. Our results indicate that the Campanian–Maastrichtian turbidites represent the first turbiditic sequence deposited after the opening of the Black Sea.

1. Introduction

Provenance studies have contributed to the tectonic and paleogeographical reconstruction of ancient to modern basins in different tectonic settings (e.g., Bracciali et al., 2016; Bussien et al., 2011; DeGraaff-Surplless et al., 2002; Gehrels, 2014; Gehrels & Dickinson, 1995).

Forearc basins are fundamental elements of active continental margins. They are short lived, and constitute the best archives that directly record information about the surrounding terranes (e.g., Dickinson, 1995; Ingersoll, 2012). As a consequence, provenance analysis of ancient forearc basins has potential to provide robust and critical constraints on the tectonic evolution of both the basin and the sediment source terranes and provide constraints on the inception and duration of the arc activity (e.g., Cawood et al., 2007; Dong et al., 2013; DeGraaff-Surplless et al., 2002; Kortyna et al., 2014; Orme et al., 2015; Sharman et al., 2015).

During the Mesozoic, the Pontides constituted the southern active margin of the Laurasia and experienced complex successive subduction-accretion events (Okay & Nikishin, 2015). The Lower Cretaceous basinal sequence in the central Pontides is represented by a submarine turbidite fan complex developed on the northern active margin of the Tethys Ocean (Akdoğan et al., 2017; Aygöl et al., 2015, 2016; Okay et al., 2006, 2013). Recently, Akdoğan et al. (2017) and Okay et al. (2013) identified detrital zircons of Archean and Paleoproterozoic ages from these turbidites. They proposed that the East European Craton north of the Black Sea was the major source for the Lower Cretaceous turbidites, pointing out that the Black Sea was not open during the deposition of the Lower Cretaceous turbidites. They concluded that, even though the Lower Cretaceous sediments were deposited above an active subduction zone (Aygöl et al., 2015,

2016; Okay et al., 2006, 2013), the related magmatic arc was not developed possibly due to flat subduction. The arc formed during the Late Cretaceous (Santonian-Campanian). Following the arc magmatism, back arc rifting and oceanic spreading took place leading to opening of the Black Sea as a back arc basin (e.g., Okay et al., 2013, 2018; Okay & Nikishin, 2015). The Upper Cretaceous (Campanian-Maastrichtian) turbidites of the central Pontides were deposited in a forearc setting following the oceanic opening of the Black Sea basin.

In this study, we report new U–Pb detrital zircon ages, petrographic data, and paleocurrent measurements from the Upper Cretaceous (Campanian-Maastrichtian) turbidites. To highlight the differences existing between turbidites deposited in the central Pontides before and after the oceanic opening of the Black Sea and also to better constrain the timing of the opening of the Black Sea, we compare our new results with those obtained by Akdoğan et al. (2017) and Okay et al. (2013) from the Lower Cretaceous turbidites.

The comparison shows a drastic change in the source–sink relation in two successive Cretaceous basin deposits in the central Pontides due to the opening of the Black Sea (Figures 1 and 2).

2. Geological Framework

The Pontides are an E–W trending mountain chain between Balkans in the west and Lesser Caucasus in the east (Figure 1). They consist of three distinct terranes named Rhodope-Strandja Massif, Istanbul Zone, and Sakarya Zone (Okay & Tüysüz, 1999; Figure 1). The Rhodope-Strandja Massif is a large crystalline terrane with Neoproterozoic metagranites (Yılmaz-Şahin et al., 2014) and Variscan quartzo-feldspathic gneissic basement intruded by Carboniferous–early Permian granitoids. This basement is stratigraphically covered by a Mesozoic metasedimentary cover (Okay et al., 2001; Sunal et al., 2006). The Istanbul Zone consists of a late Neoproterozoic granitic and metamorphic basement (Chen et al., 2002), covered by a continuous sedimentary succession from Ordovician to Carboniferous (Özgül, 2012). The Istanbul Zone is separated from the Rhodope-Strandja Massif by the dextral strike-slip West Black Sea Fault, and from the Sakarya Zone in the south by the Intra Pontide Suture Zone (Okay & Tüysüz, 1999). The Sakarya Zone, with its 1,500-km length, is the largest continental fragment of the Pontides (Figure 1). The basement of the Sakarya Zone is made up of metamorphic basement intruded by Devonian, Carboniferous, and Permian granites (e.g., Dokuz, 2011; Nzegge et al., 2006; Sunal, 2013; Topuz et al., 2010; Ustaömer et al., 2012, 2013). The Pontides are separated from the Tauride-Anatolide Platform in the south by the Izmir–Ankara–Erzincan suture Zone (Figure 1).

During the late Paleozoic and Mesozoic the Pontides formed the active margin of Laurasia facing the Tethys Ocean to the south. Magmatic arcs and subduction accretion complexes of Permo-Carboniferous, Late Triassic, Middle-Late Jurassic, and Early and Late Cretaceous ages document a long history of northward subduction under Laurasia (Okay & Nikishin, 2015). Between these magmatic events, a large submarine turbidite basin formed in the central Pontides during the Early Cretaceous. In contrast to the presence of the Early Cretaceous subduction-accretion complexes indicating northward subduction of the Tethys Ocean during deposition of this turbidites (Aygül et al., 2015; Okay et al., 2006, 2013), there is no evidence for a contemporaneous arc magmatism, possibly due to flat subduction (Akdoğan et al., 2017; Okay et al., 2013). During the Late Cretaceous an extensive submarine arc magmatism took place and the Black Sea back-arc basin opened as a result of rifting of the Pontide magmatic arcs, thereby separating the Laurasia from the Pontides (e.g., Akdoğan et al., 2017; Okay et al., 2013, 2018; Tüysüz, 1999, 2018).

In the central Pontides, the basement of the Sakarya Zone consists of Hercynian metamorphic rocks with Permo-Carboniferous granites (Nzegge et al., 2006; Okay et al., 2013) and Upper Triassic distal turbidites forming part of an accretionary complex (Ustaömer & Robertson, 1994; Figure 3). These are overlain and intruded by Middle-Upper Jurassic acid to intermediate volcanic and subvolcanic rocks of the Jurassic arc (Nzegge, 2008; Okay et al., 2013, 2014; Yılmaz & Boztuğ, 1986). Middle Jurassic (approximately 160 Ma) accretionary complexes consisting of blueschist to lower greenschist facies metamorphic rocks, crop out in the central Pontide Supercomplex (Aygül et al., 2016; Frassi et al., 2018; Marroni et al., 2014; Okay et al., 2013, 2014) indicating an active tectonic setting. A major part of the central Pontide Supercomplex in the southern central Pontides consists of eclogites, blueschists with oceanic protoliths and with Early Cretaceous phengite Ar–Ar ages of 136–102 Ma, indicating northward subduction of Tethys at this period



Figure 1. The main tectonic units of Black Sea region showing depositional area of the Lower Cretaceous and Campanian-Maastrichtian sequences in the Pontides and the Upper Cretaceous magmatic arc. The red rectangle shows the study area. CPS, Central Pontide Metamorphic Complex; WBS Fault, Western Black Sea Fault (modified from Akdoğan et al., 2017 and Okay et al., 2013).

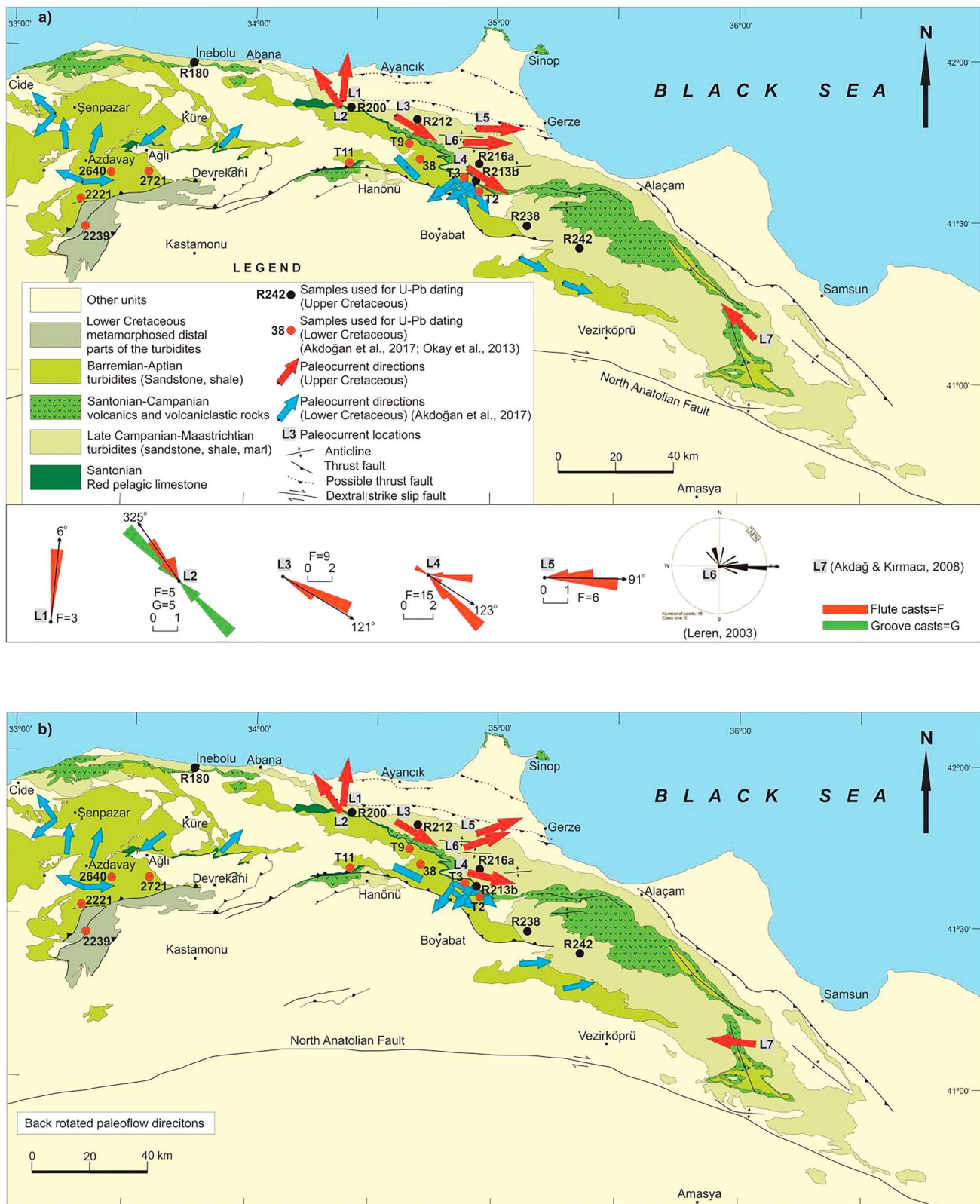


Figure 2. Geological maps of the central Pontides showing the distribution of the Lower Cretaceous and Campanian-Maastrichtian turbidites, the paleocurrents, and sample locations used for U–Pb dating (modified after Akdoğan et al., 2017; Hakyemez & Papak, 2002; Uğuz et al., 2002). (a) Paleoflow directions of the Campanian-Maastrichtian turbidites are from this study, Leren (2003), and from Akdağ and Kırmacı (2008) and those of the Lower Cretaceous turbidites are from Akdoğan et al. (2017). (b) All paleoflow directions were back-rotated according to Meijers et al. (2010).

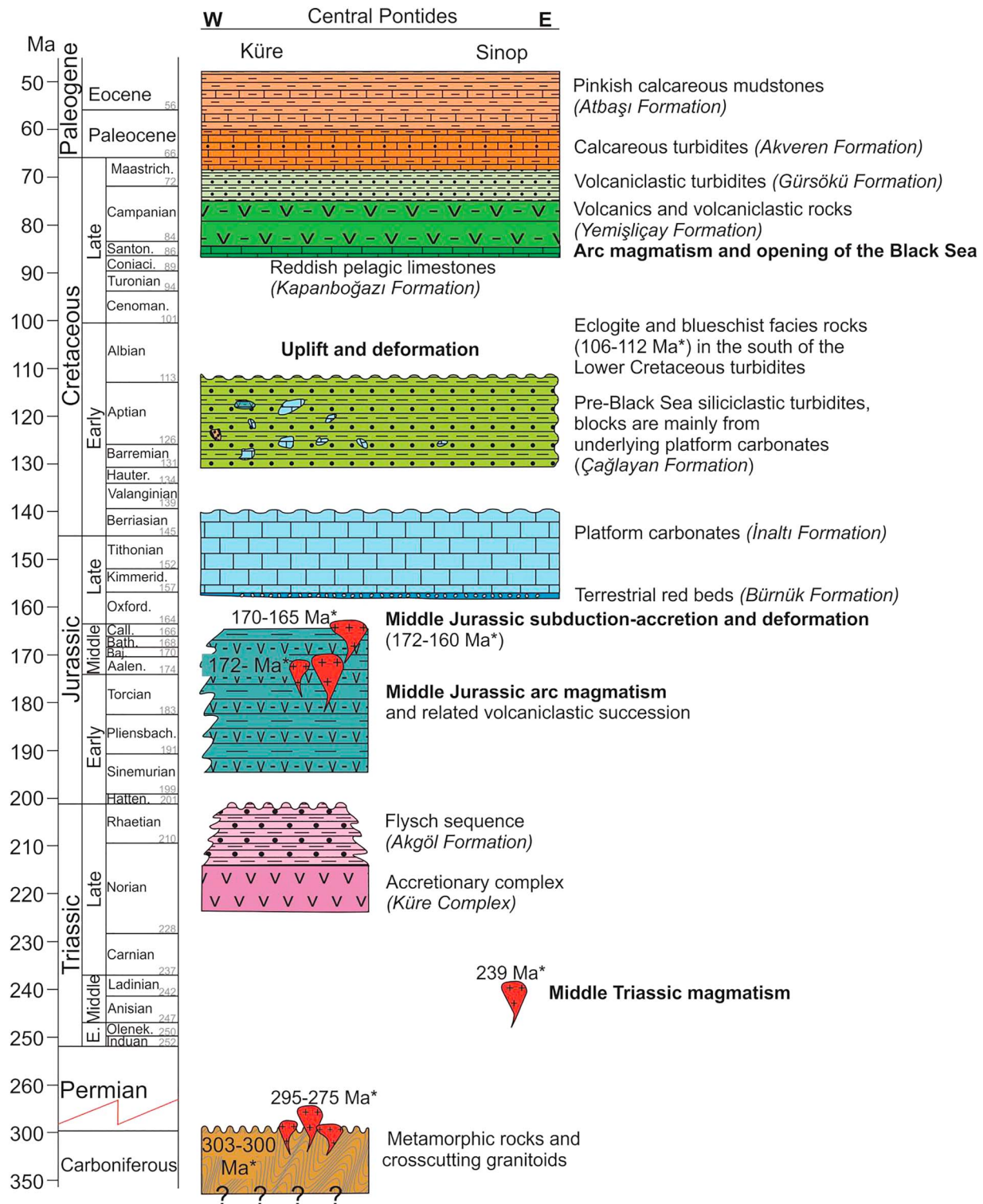


Figure 3. Generalized chrono-stratigraphic chart of the north-eastern part of the central Pontides; modified from Akdoğan et al. (2017). The time scale is from Gradstein et al. (2012). Isotopic ages are from Ballato et al. (2018), Nzege (2008), Nzege et al. (2006), and Okay et al. (2013, 2014). In this study detrital zircons from the Gürsöku formation were studied.

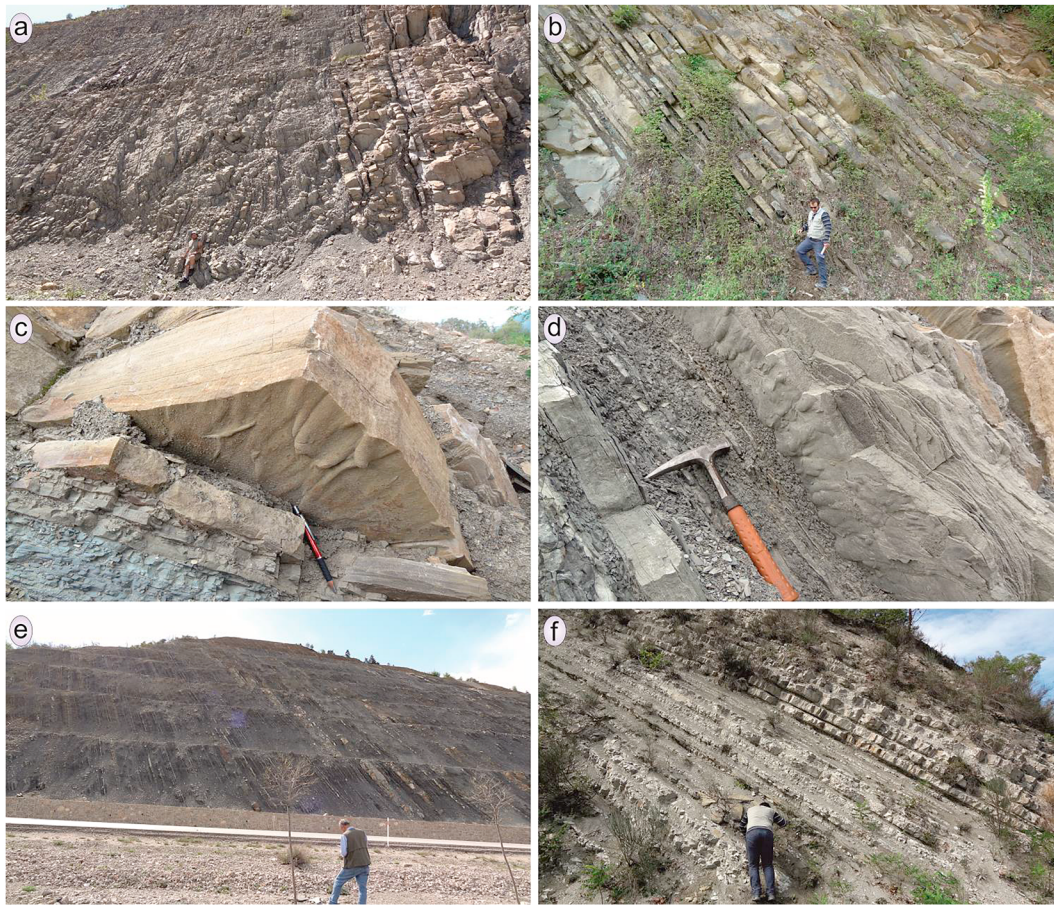


Figure 4. Field photographs of the Campanian-Maastrichtian turbidite sequence of the central Pontides. (a and b) Medium-thickly bedded sandstones interbedded with thin marl layers (Durağan and Gökçealan). (c) Flute casts indicating the paleocurrent direction from west to east (Boyabat). (d) Fine-grained sandstone and marl alternation showing thin graded bedding in the base level of the sandstones and flute casts at the sandstone layers (Boyabat). (e) Thin-bedded sandstone shale alternation showing the distal parts of turbidites (Boyabat). (f) Medium-bedded calciturbidites of Maastrichtian to Paleocene age (Akveren formation; Yeşiloba Village).

(Aygül et al., 2015, 2016; Okay et al., 2006, 2013; Figure 3). The Triassic and Jurassic series are unconformably overlain by a thick sequence of Upper Jurassic-lowermost Cretaceous (Kimmeridgian-Berriasian) shallow marine limestones, which extends throughout the Pontides and beyond (Okay et al., 2018). The limestones are in turn unconformably covered by thick (>2,000 m), extensive Lower Cretaceous (Barremian-Aptian) siliciclastic turbidites consisting mainly of intercalated medium-grained sandstone and shale (Akdoğan et al., 2017; Hippolyte et al., 2010; Tüysüz, 1999).

An important change in the sedimentation occurred in the Santonian with the deposition of red pelagic limestones, which lie unconformably over the older stratigraphic units. The red pelagic limestones, possibly represent the breakup unconformity and the initiation of the oceanic spreading in the Black Sea basins (Görür, 1988; Görür et al., 1993), and are associated with volcanic rocks (Hippolyte et al., 2010, 2016; Okay et al., 2013, 2018; Tüysüz et al., 2016). Arc volcanism started in the Coniacian and continued into Campanian (Figure 3). Deep seismic reflection studies indicate that the Upper Cretaceous volcanoes exist under the Black Sea close to the Turkish coastline (Nikishin et al., 2015). Volcaniclastic turbidite sequences with a thickness up to 1,200 m were deposited in a forearc basin south of the Upper Cretaceous arc. These Campanian-Maastrichtian turbidites of the central Pontides (the Gürsöku Formation; Figure 3) comprise graded volcaniclastic sandstones interbedded with shale, calcareous mudstones, and marlstones (Ellero et al., 2015; Leren et al., 2007) and extend further east to the Eastern Pontides (Okay & Şahintürk, 1997; Figures 1 and 4a–4e). These sheet-like turbidites indicate nonchannelized low- to high-density storm-

generated flow and forming an upward thinning, transgressive stratigraphic succession (Leren et al., 2007; Figures 4a–4e). Time-equivalent calciturbiditic sequences were deposited in the Western Pontides (Özcan et al., 2012).

Nannofossils and foraminiferal content constrain the depositional age of this volcanoclastic turbiditic sequence to the Campanian-Maastrichtian (Aydın et al., 1986; Gedik & Korkmaz, 1984; Hippolyte et al., 2016; Leren et al., 2007; Okay et al., 2018; Özcan & Özkan-Altın, 1999; Özkan-Altın & Özcan, 1999; this study). The turbidites become gradually more calcareous upward and pass into white deep-marine marl and calciturbidites of Akveren formation with depositional ages of Maastrichtian to Paleocene (Aydın et al., 1986; Leren et al., 2007; Okay et al., 2018; Figures 3 and 4f).

The collision between the Pontides and the Kırşehir Massif occurred during the Paleocene–Eocene resulting in uplift and deformation (Okay & Tüysüz, 1999) and oroclinal bending (Meijers et al., 2010) of the central Pontides. The northern part of the central Pontides forms a north-vergent fold-and-thrust belt of Eocene age. Espurt et al. (2014) proposed approximately 28 km of shortening in a north-south direction by the end of Eocene, as a result of collision of the Kırşehir Massif with the Pontides. The Campanian-Maastrichtian turbidites, along with the rest of Mesozoic-Paleocene sequence, were folded and thrust faulted. However, the sequence maintains stratal continuity (Figure 4).

3. Materials and Methods

We document new paleoflow directions from the Campanian-Maastrichtian turbidites that are given in Table S1. At each locality all accessible paleocurrent indicators were recorded, and correction for tectonic tilting was applied during the measurement for dips higher than 10°. The mean paleocurrent direction values were obtained by using the Stereonet 9.5 software (Allmendinger et al., 2011).

Campanian-Maastrichtian turbidites were sampled for U–Pb zircon dating and petrography. Mesoscopic features of the sampled turbidites with field photographs are given as Text S1 and Figure S1 in the supporting information. Detailed petrographic descriptions of seven dated Campanian-Maastrichtian sandstone samples are given in Text S2 and Figures S2–S7 in the supporting information. Framework compositions of the dated Campanian-Maastrichtian samples were determined by point counting ($n > 500$) according to the Gazzi-Dickinson method (Dickinson, 1970; Gazzi, 1966; Zuffa, 1985). Point counting results are shown in Tables S2 and S3 in the supporting information. Heavy mineral separation was performed using standard techniques (Text S3 in the supporting information).

Zircon is a heavy mineral resistant to geological processes, and a common accessory detrital mineral in siliciclastic sediments (e.g., Fedo et al., 2003). Thus, detrital zircon U–Pb geochronology is widely used as an important tool for deciphering the provenance of the sediments as well as for revealing the tectonic and paleogeographical context of the basins and surrounding regions (e.g., Bussien et al., 2011; DeGraaff-Surpless et al., 2002; Gehrels & Dickinson, 1995). In this study, we determined the U–Pb ages of the detrital zircons from the Campanian-Maastrichtian samples using laser ablation ICP-MS technique to constrain the tectonic history of the Cretaceous basins in the Black Sea region. Analytical procedure for U–Pb dating is given in Text S3 in the supporting information, and all analytical results are listed in Table S4. The Campanian-Maastrichtian sandstone samples used for U–Pb dating were collected from different parts and levels of the >1,200-m-thick succession over a northwest-southeast distance of 300 km (Figure 2). The UTM coordinates of the samples are given in Table S4, and their locations are shown in the geological map in Figure 2. The precise stratigraphic positions of the samples within the Campanian-Maastrichtian sequence are therefore not known, except R-213b, which comes from the upper parts of the succession and is rich in calcareous components. Sandstones are characterized by gray color. The layer thicknesses range from 5 to 50 cm. The percentage of the sandstone-shale is quite variable (Figure 4).

Some of the Lower Cretaceous sandstone samples from the central Pontides, which were dated for detrital zircons in Akdoğan et al. (2017) and Okay et al. (2013), were also point counted to compare the petrographic features of the two different turbiditic sequences. The point counting results of the studied Lower Cretaceous samples are shown in Tables S2 and S3 in the supporting information with petrographic descriptions in Akdoğan et al. (2017) and Okay et al. (2013).

4. Results

4.1. Paleocurrent Measurements

Forty-three paleocurrent measurements were made using mainly unidirectional indicators from 38 flute casts and bidirectional (linear) indicators from five groove casts from five locations through the Campanian-Maastrichtian sequence (Figure 2 and Table S1). Paleoflow direction L6 is from Leren (2003) and L7 is from Akdağ and Kırmacı (2008).

The central Pontides form a broad arc, which was produced through oroclinal bending clockwise and counterclockwise rotation with angles of up to 40°, during the Late Cretaceous to Eocene as a result of continental collision with the Kırşehir Massif (Meijers et al., 2010). Due to the oroclinal bending of the central Pontides the vector mean values of the measured paleocurrent directions were back rotated according to data in Meijers et al. (2010), to establish initial directions of the paleocurrents (Figure 2 and Table S1). These back rotated paleoflow directions are used for interpretation (Figure 2).

Paleocurrent measurement L1, L2, and L3 were not affected by rotation due to their position in the apex of the orocline (Meijers et al., 2010). Counterclockwise back rotations of 20° were applied for locations L4 and L5. Counterclockwise back rotations of 20° and 40° were applied to paleoflow directions from locations L6 (Leren, 2003) and L7 (Akdağ & Kırmacı, 2008), respectively. However, there is no major change between most of the nonrotated and back rotated paleocurrent directions due to low rotation angles (Meijers et al., 2010). Location L7 is exceptional with its high counterclockwise back rotation angle of 40°, indicating paleoflow direction that is semiparallel to axis of the basin (Figure 2).

Corrected paleocurrents from Campanian-Maastrichtian turbidites are predominantly northwest to southeast and southeast to northwest, showing that the dominant transport was axial and parallel to the axis of the basin.

4.2. Sample Petrography

The detailed description of the individual Campanian-Maastrichtian sandstone samples and the point counting results are given in Texts S1 and S2; Tables S2 and S3; and Figures 5, 6, and S1–S7. According to modal compositions Campanian-Maastrichtian samples can be classified mainly as lithic arenite (Folk et al., 1970). They are moderately to poorly sorted with subangular to angular grains (Figures S2–S7). The Campanian-Maastrichtian samples contain abundant (26–39% vol.) detrital carbonate grains of variable size and abundant magmatic lithic grains (13–28% vol.; Figures 5, 6, and S1–S6; Text S2; and Tables S2 and S3). Sample R-213b is exceptional, since in that micritic limestone grains and microfossils make up 65% of the rock volume (Figures 5, 6, and S3). Planktonic foraminiferal assemblages in this sample indicate a middle Campanian-early Maastrichtian age range based on the presence of *Globotruncana linneiana*, *Globotruncana ventricosa*, *Globotruncana arca*, *Gansserina gansseri*?, and *Pithonella ovalis*. The lithic fragments in the Campanian-Maastrichtian sandstones consist mainly of sedimentary rock fragments (28–42% vol.), felsic-mafic volcanic-plutonic clasts (13–28% vol.), and minor amounts of metamorphic clasts (<10% vol.; Figure 6a). Fresh and altered feldspar grains are also present (up to 20% vol. in sample R-242 and <14% vol. in other samples). Quartz occurs both as monocrystalline and polycrystalline quartz aggregates, ranging 6–37% vol. Notable detrital accessory minerals include epidote, muscovite, and biotite.

Petrographic descriptions of the Lower Cretaceous sandstone samples, on which point counting performed during this study (Tables S2 and S3 and Figure 6), were documented by Akdoğan et al. (2017) and Okay et al. (2013). On the conventional QFL ternary discrimination diagram (Dickinson et al., 1983), the Campanian-Maastrichtian samples overlap the dissected to undissected arc provenance fields, whereas the Lower Cretaceous samples lie in the recycled orogenic provenance field (Figure 6b and Table S3).

4.3. U–Pb Ages of Detrital Zircons

A total of 779 U–Pb ages were determined on detrital zircon grains from seven Campanian-Maastrichtian turbiditic sandstone samples of the central Pontides (Figure 2, Text S3, and Table S4). Most of the zircons are euhedral and exhibit well-developed crystal faces and well-preserved oscillatory growth zoning in CL images (Corfu, 2003). Their sizes range between 60 and 250 μm with length/width ratio approximately 2:1. Representative CL images of the detrital zircon grains for each sample are given in Figure 7. 632 zircon grains (81% of the total population) provided concordant U–Pb ages (at 90–110% level) and are used in this

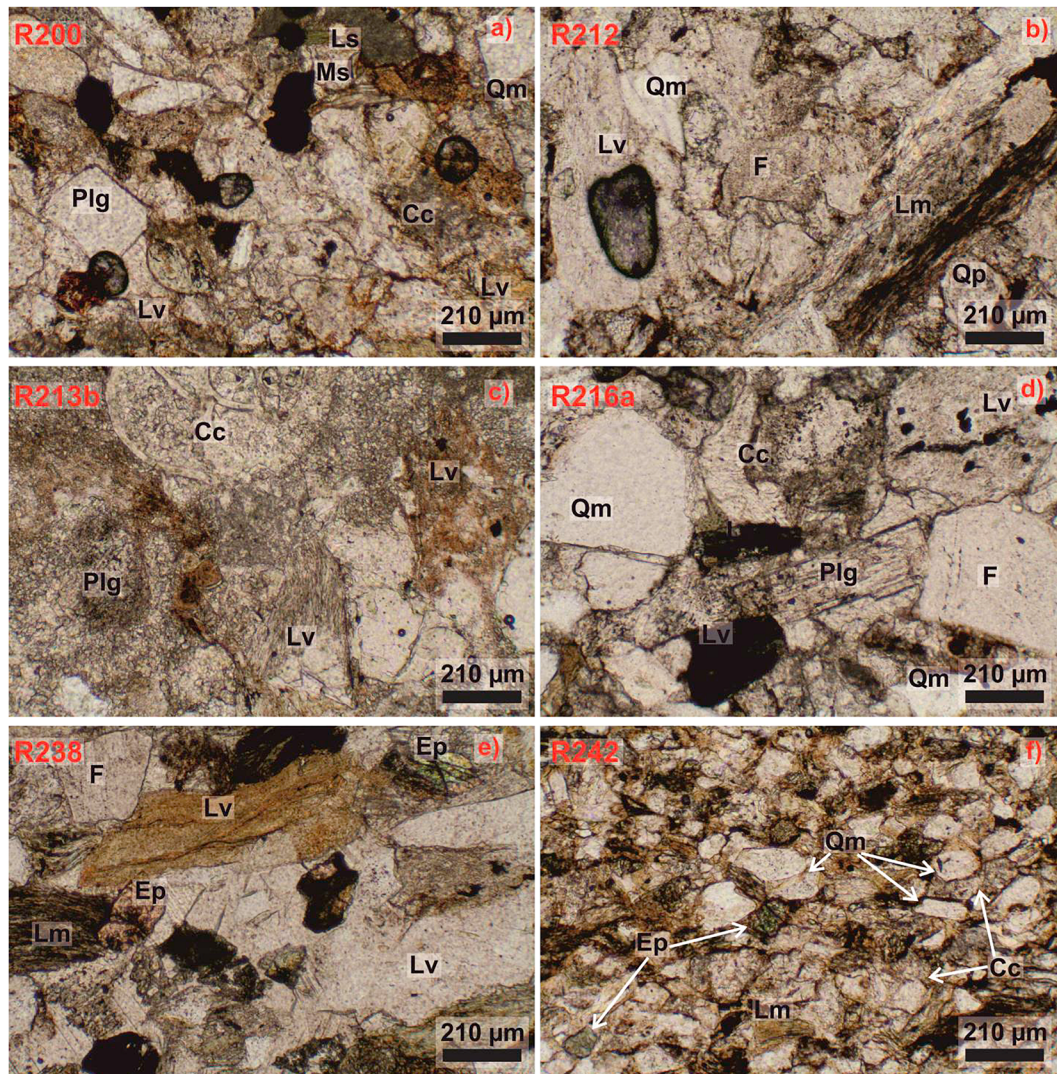


Figure 5. Photomicrographs of the Campanian-Maastrichtian samples in plane-polarized light. (a) Volcanic lithic fragments with euhedral plagioclase grain and elongate muscovite surrounded by calcite fragments showing short transport distance. (b) Large metamorphic rock fragment with volcanic rock clast, quartz grains, and calcite fragments indicate crystalline rock sources. (c) Mainly calcite fragments with minor volcanic and metamorphic lithic clast and plagioclase grain replaced by calcite indicating the upper part of the succession passing into the claciturbidites of Akveren formation. (d) Large mono-crystalline quartz and feldspar with euhedral fresh plagioclase, volcanic lithic fragments, and calcite fragments indicating granitic sources and short transport distance from the source rocks. (e) Metamorphic rock fragments, volcanic rock clasts, and polycrystalline quartz and epidote grains with high relief indicate crystalline basement sources. (f) Fine-grained sandstone with monocrystalline quartz and epidote grains surrounded by calcite clasts suggest crystalline basement as the source rocks. Monocrystalline quartz (Qm), polycrystalline quartz (Qp), feldspar (F), plagioclase (Plg), volcanic rock fragment (Lv), metamorphic rock fragment (Lm), sedimentary rock fragment (Ls), epidote (Ep), muscovite (Ms), and calcite (Cc).

study. The Th/U values of the detrital zircons range from 0.01 to 2.26 (Figure 8 and Table S4). In particular, 93% are in range of 0.1–1.5, 3% are <0.1, and 3% are in range of 1.5–2.0 and only a few zircons (<1%) have Th/U values >2 (Figure 8). The detrital zircon ages are mainly Mesozoic (49%) and Paleozoic (35%), with minor Neoproterozoic zircons (10%; see Figures 8 and 9). Mesoproterozoic-Archean zircons are rare (6% of the cumulative age population).

Based on the age results, the samples can be subdivided into three groups in terms of detrital zircon ages. Samples R200, R213b, and R216a yielded similar Campanian age components (Figures 10 and 11). Sample R212 shows a prominent component at 180–160 Ma (Middle Jurassic; 48%). Zircons from samples R180, R238, and R242 show a more dispersed age distribution, with two major clusters of Carboniferous (approximately 330 Ma) and Permian (approximately 255 Ma) ages, corresponding to the 49%, 37%, and 41% of the

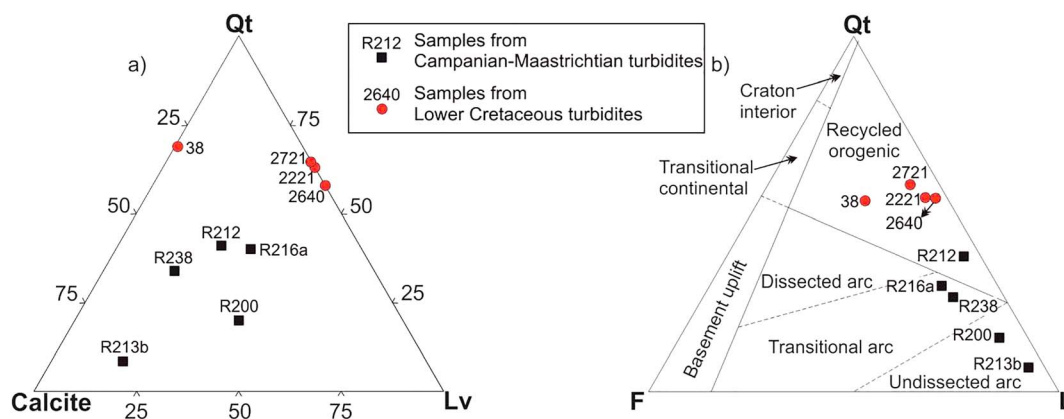


Figure 6. Sandstone samples from Lower Cretaceous and Campanian–Maastrichtian turbidites plotted on the (a) lithic and quartz component and (b) tectonic discrimination ternary diagrams (Dickinson et al., 1983). Qt, mono and polycrystalline quartz; F, feldspars (K-feldspar and plagioclase); L, total lithic grains; Lv, volcanic lithic grains.

cumulative age population, respectively (Figure 10). Two of these samples include major Triassic (250–220 Ma) age components.

5. Discussion

5.1. Provenance of the Upper Cretaceous (Campanian–Maastrichtian) Turbidites of the Central Pontides

Detrital zircon ages of the Campanian–Maastrichtian turbidites of the central Pontides (the Gürsöku formation) cluster around Paleozoic to Mesozoic (84% of all concordant data) and to a minor extent in the Neoproterozoic (10%; Figure 9). Mesoproterozoic–Archean zircons make up only 6% of the total zircon population without any significant peak. The Late Cretaceous zircons with a Campanian age cluster (approximately 79 Ma; Figure 11) make up 63% of all Mesozoic zircons. The Th/U values as a proxy is used to discriminate igneous and metamorphic zircons, with a ratio of 0.1 forming the boundary between zircons from igneous origin (higher values) and metamorphic origin (lesser values; Hoskin & Schaltegger, 2003; Rubatto, 2002). The 97% of the detrital zircons from Campanian–Maastrichtian sandstones have Th/U values >0.1 (Figure 8 and Table S4). CL images of the internal structures of the detrital zircons also provide important clues about their origin (e.g., Corfu, 2003). Most of zircons from the Campanian–Maastrichtian turbidites are remarkably euhedral and show clear oscillatory zonation in CL images (Figure 7); this, together with their Th/U values >0.1 (Figure 8 and Table S4), suggests magmatic origin for most of the detrital zircons. These zircons were, thus, derived from the coeval Upper Cretaceous magmatic arc, which is generally represented by submarine volcanic and volcanoclastic rocks and can be traced continuously along the Pontides (e.g., Keskin & Tüysüz, 2018; Okay & Nikishin, 2015; Tüysüz, 2018). This interpretation is supported also by the sandstone framework compositions. The proportion of volcanic-plutonic clasts reaches 27% vol. and single feldspar grains up to 13% vol. in Campanian–Maastrichtian sandstone samples (Tables S2 and S3). The petrographic compositions of the Campanian–Maastrichtian turbiditic sandstone samples along with the abundance of Coniacian–Campanian detrital zircon ages (30%; Figure 11 and Table S4) indicate sediment derivation chiefly from local volcanic and plutonic sources; the lithic grains can be counted mainly as neovolcanic clasts (according to the criteria of Critelli & Ingersoll (1995)). The nearest dated parts of the Upper Cretaceous volcanic arc are in the Sinop area, with Ar–Ar ages on biotite grains of 79 to 72 Ma (Aydınçakır, 2016; Figure 2). Zircons from felsic tuffs layers in the Campanian–Maastrichtian volcanoclastic turbidites from the Eastern Pontides yielded U–Pb zircon ages in the range of 84–71 Ma (Eyüboğlu, 2015) similar to the detrital zircons reported here. Arc-related plutons in the Eastern Pontides have U–Pb zircon ages of 86–70 Ma (e.g., Delibaş et al., 2016; Karsli et al., 2010, 2012; Kaygusuz et al., 2008, 2014; Kaygusuz & Şen, 2011; Özdamar, 2016) and with the K–Ar mica ages of 84–71 Ma in the Strandja Zone in the west (Moore et al., 1980; Ohta et al., 1988).

The Jurassic detrital zircons, clustering around 165 Ma, make 10% of total concordant ages. It is most pronounced in sample R212 (Figure 10), indicating that the Jurassic granitoids and acid volcanic rocks in the

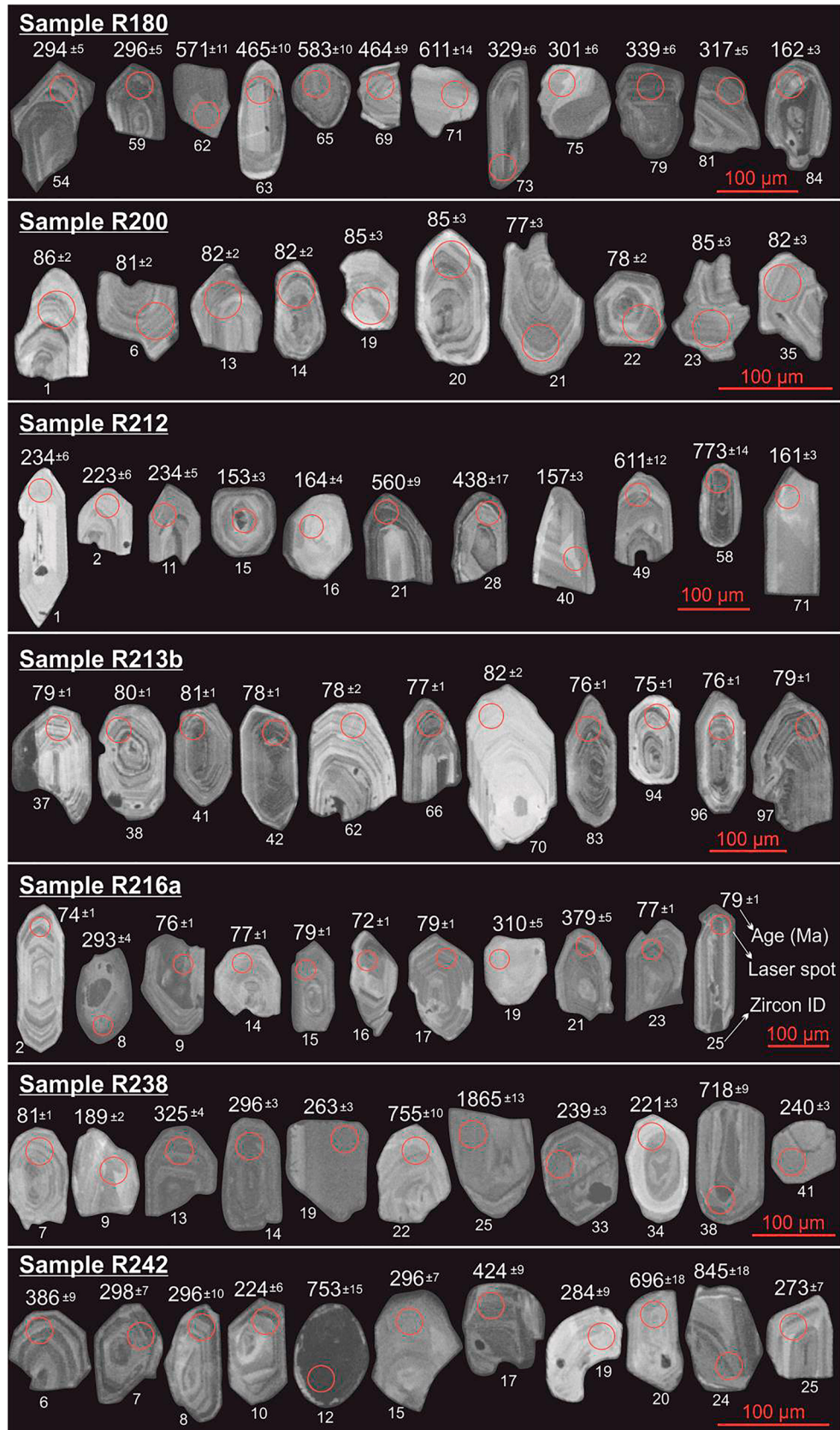


Figure 7. CL images, spot locations, and the U-Pb ages of the representative detrital zircons of the Campanian-Maastrichtian sandstone samples.

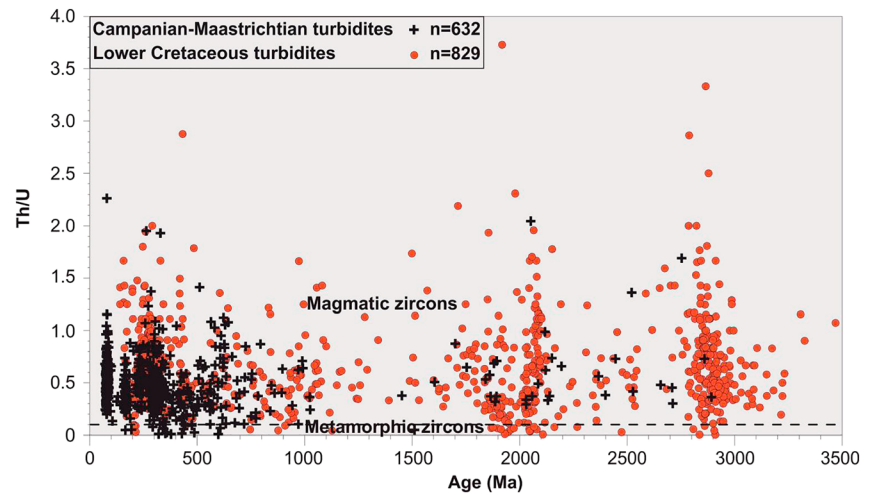


Figure 8. Th/U ratio versus U-Pb ages of the detrital zircons from Campanian-Maastrichtian (this study) and Lower Cretaceous sandstone samples (Akdoğan et al., 2017; Okay et al., 2013). Discrimination line is from Rubatto (2002).

central Pontides (Nzegge, 2008; Okay et al., 2013, 2014; Yılmaz & Boztuğ, 1986) were locally feeding the Campanian-Maastrichtian turbidites.

Triassic detrital zircons constitute 8% of the total detrital zircon population of the Campanian-Maastrichtian turbidites (Figure 10). Triassic magmatic rocks are not known in the Pontides, except for a newly reported small intrusion of approximately 240 Ma from the central Pontides (Ballato et al., 2018). An E-W trending subsurface Triassic magmatic arc is thought to exist in the Scythian Platform beneath the Tertiary sediments (Okay et al., 2013; Okay & Nikishin, 2015). However, derivation of the Triassic zircons from the Triassic magmatic arc to the north is unlikely since during the deposition of Campanian-Maastrichtian turbidites, the Black Sea was already open hindering the connection between the Pontides and the Scythian Platform. Possibly the Triassic zircons were recycled from the Paleo-Tethyan subduction accretion complexes of the Pontides which are dominated by the Triassic zircons (Karşlıoğlu et al., 2012; Ustaömer et al., 2016).

Carboniferous-Permian zircons (359–252 Ma) make up 25% of the analyzed zircons. Most of them cluster in the range of 330–290 Ma (late Carboniferous-early Permian; 57%). This age range is similar to the ages of the magmatic bodies from the Sakarya Zone and the Lesser Caucasus (e.g., Nzegge, 2008; Nzegge et al., 2006;

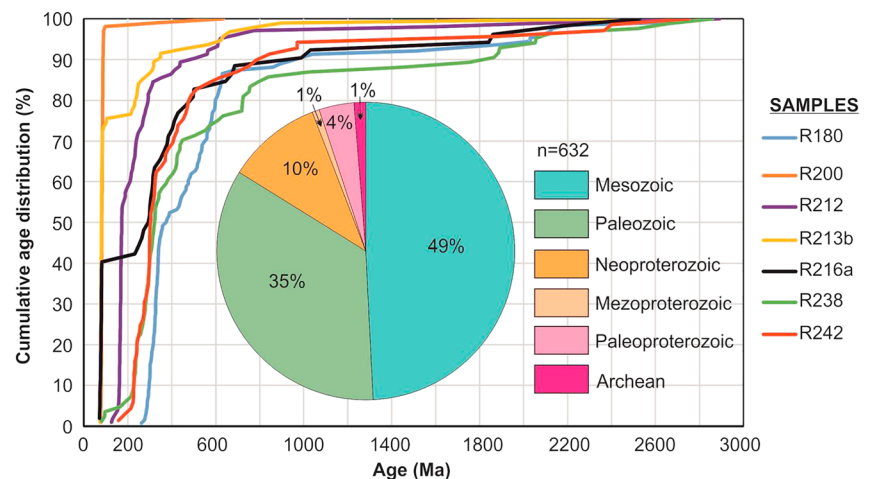


Figure 9. Cumulative distribution of concordant U-Pb ages of detrital zircons from the Campanian-Maastrichtian turbidites. The pie chart shows distribution of all detrital zircon ages to the geological eras.

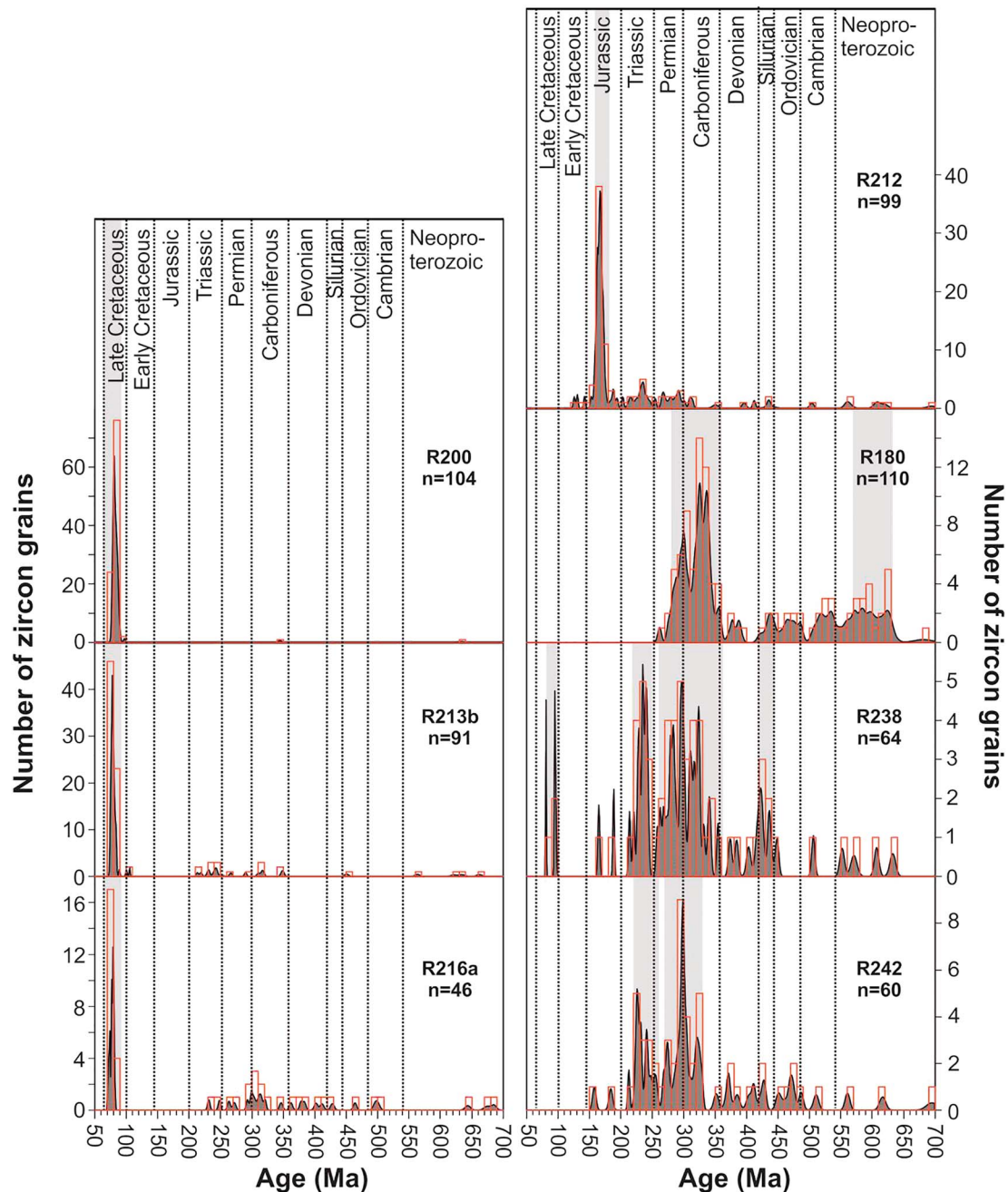


Figure 10. Age histogram with probability density curves of seven samples from the Campanian-Maastrichtian turbidites of the central Pontides. Only ages below 700 Ma are shown. The gray columns show the main clusters.

Mayringer et al., 2011; Topuz et al., 2007, 2010; Ustaömer et al., 2012, 2013). The closest outcrops are the Deliktaş and Sivrikaya granites in the central Pontides, with U–Pb zircon ages of 303–275 Ma (Nzegge et al., 2006). Late Carboniferous to Permian granitoids are also common in the Strandja Massif and in the Balkanides with U–Pb zircon age range of 315–250 Ma (e.g., Carrigan et al., 2005; Sunal et al., 2006, 2008). Although Early Carboniferous granites of 359–330-Ma ages are not known in the Pontides or in the Black Sea region, detrital zircons of this range make 30% of the Carboniferous zircons in the Campanian-Maastrichtian turbidites. Detrital zircons of Early Carboniferous age are also common in the Carboniferous turbidites (Okay et al., 2011), in the Lower Cretaceous shelf clastics and in the turbidites in the western part of the Lower Cretaceous basin (Akdoğan et al., 2017). Consequently, they may have been

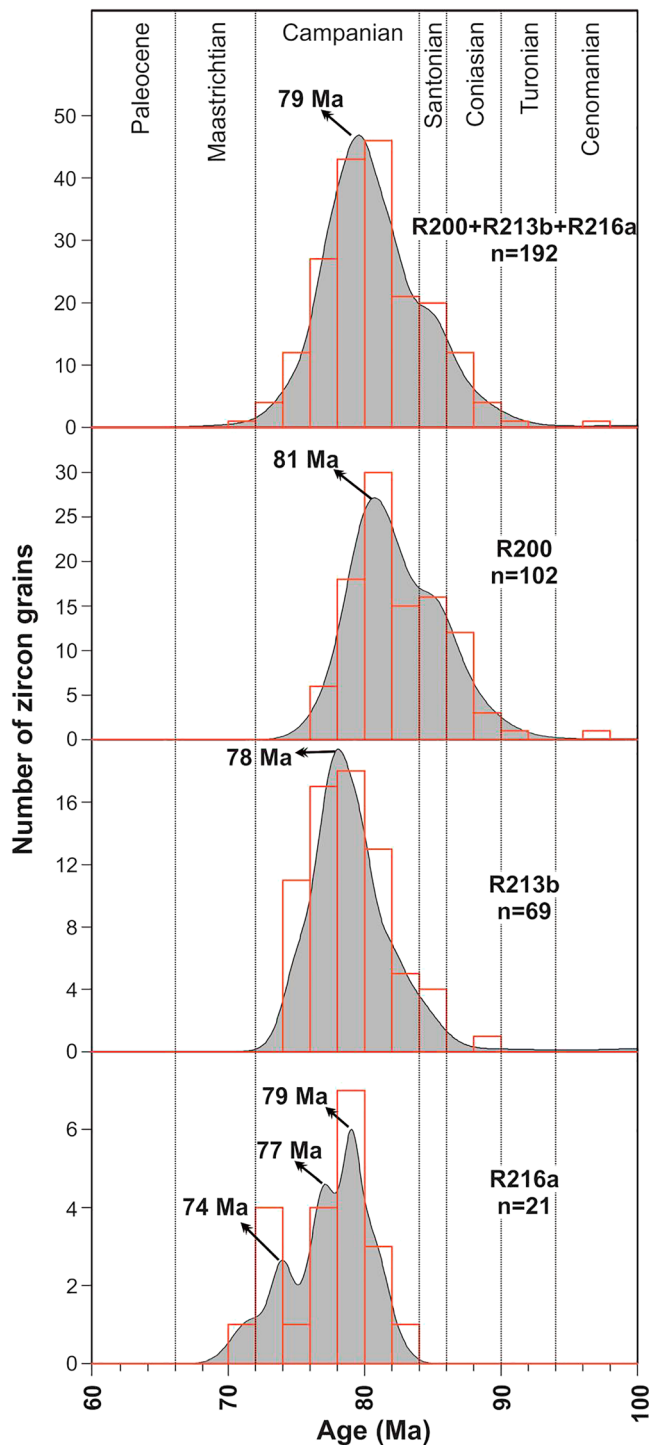


Figure 11. (a) Age histogram showing the Late Cretaceous zircon distributions combined from three Campanian-Maastrichtian sandstone samples of R200, R213b, and R216a. (b–d) The Late Cretaceous zircon distributions from the individual samples of R200, R213b, and R216a, respectively.

the recycled orogenic field and the Campanian-Maastrichtian turbidites in the magmatic arc field (Figure 6b).

The detrital zircon age distributions of the Lower and Upper Cretaceous (Campanian-Maastrichtian) sandstones of the central Pontides are also significantly different (Figure 12). The detrital zircon age distribution

recycled into the Campanian-Maastrichtian sandstones. This constitutes supportive data that the Istanbul and Sakarya Zones were amalgamated before the Cretaceous, most probably before the Late Jurassic (e.g., Akdoğan et al., 2017; Cavazza et al., 2012; Okay et al., 2013, 2018). Variscan and Jurassic metamorphic rocks (e.g., Gücer et al., 2016; Okay et al., 2013; Topuz et al., 2007) were likely the sources of the metamorphic rock fragments and epidote grains found in the Campanian-Maastrichtian sandstones.

In summary, abundant volcanic-plutonic fragments (up to 27%) and single-feldspar grains (mainly plagioclase; up to 13%) from neovolcanic sources (Critelli & Ingersoll, 1995), the U–Pb detrital zircon age distribution, and paleocurrent directions imply that the Late Cretaceous forearc basin was sourced mainly from the penecontemporaneous Upper Cretaceous magmatic arc.

5.2. Opening of the Black Sea and Provenance of the Cretaceous Turbidites

Provenance analysis on the Lower Cretaceous turbidites indicates that the eastern, central, and western parts of the basin were fed from different source rocks (Akdoğan et al., 2017). The majority of the U–Pb detrital zircon ages in the central and eastern parts of the Lower Cretaceous basin are Archean and Paleoproterozoic (Akdoğan et al., 2017; Okay et al., 2013). In contrast, the western part of the Lower Cretaceous basin is dominated by Carboniferous and Neoproterozoic zircons (Akdoğan et al., 2017). To make comparison with Campanian-Maastrichtian turbidites deposited in the eastern part of the central Pontides, we focused on the detrital zircon data from the eastern and central parts of the Lower Cretaceous basin, where our Campanian-Maastrichtian samples were collected (Figures 1 and 2). Petrographic compositions, paleoflow directions, and detrital zircon ages of these two Cretaceous turbiditic successions of the central Pontides are markedly different. Here we compare all the available data from these two turbiditic successions.

According to petrographic observations, the Campanian-Maastrichtian turbidites are rich in calcite (>30% vol. in general and 65% vol. in sample R-213b) and magmatic rock fragments (up to 27% vol.; Text S2, Tables S2 and S3, and Figures S2–S7) in contrast to those of Lower Cretaceous turbidites, which are dominated by quartz (>47% vol.) and fresh microcline grains in some samples (Figures 5 and 6 and Tables S2 and S3; see also Akdoğan et al., 2017). Abundant volcanic-plutonic rock fragments, plagioclase grains, and Coniacian-Campanian detrital zircons (30%; Table S4 and Figures 5, 10, 11, and S1–S6) in the Campanian-Maastrichtian sandstones suggest coeval or slightly older magmatic sources for the Campanian-Maastrichtian turbidites. The Lower Cretaceous turbidites have relatively lesser amounts of carbonate fragments (<15% vol.) and are enriched in quartz (>45% vol.) and K-feldspar (mainly microcline, up to 7% vol. in some samples; Figure 6 and Tables S2 and S3) and contain abundant Archean-Mesoproterozoic zircons (57%; Figure 12; Akdoğan et al., 2017; Okay et al., 2013). In the QtFL tectonic discrimination diagram of Dickinson et al. (1983), the Lower Cretaceous turbidites plot in

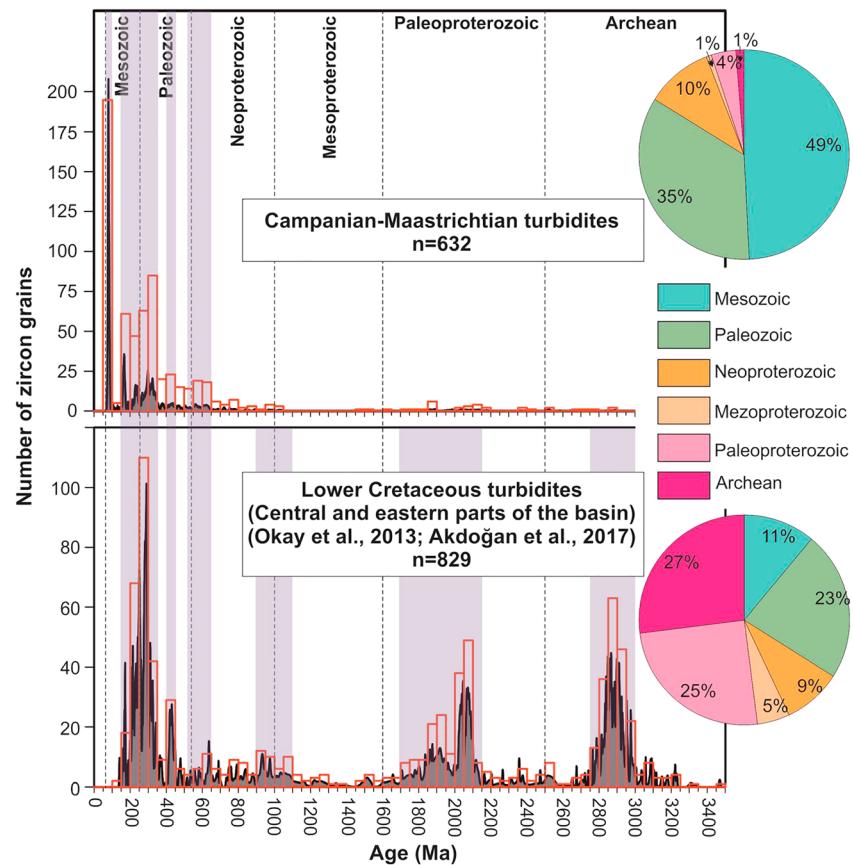


Figure 12. Age histograms and pie charts showing the U–Pb detrital zircon ages from the Campanian-Maastrichtian turbidites (this study) and Lower Cretaceous turbidites (Akdoğan et al., 2017; Okay et al., 2013) emphasizing the significant differences.

of the Lower Cretaceous turbidites from the eastern part of the central Pontides is dominated by Archean, Paleoproterozoic, and Mesoproterozoic zircons (57%; Akdoğan et al., 2017; Okay et al., 2013), whereas zircons from the Campanian-Maastrichtian turbidites exhibit prominent peaks at Late Cretaceous (mainly Campanian) and at Late Carboniferous with a very small percentage (6%) of Archean, Paleoproterozoic, and Mesoproterozoic zircons. The absence of exposed Archean–Paleoproterozoic rocks in the Pontides and their presence north of the Black Sea indicate that the Lower Cretaceous turbidites of the eastern part of the central Pontides were mainly sourced from the Ukrainian Shield (Akdoğan et al., 2017; Okay et al., 2013; Figure 13a), where Archean and Paleoproterozoic basement rocks crop out widely (e.g., Bibikova et al., 2008, 2015; Bogdanova et al., 2008, 2010; Claesson et al., 2006; Shchipansky & Bogdanova, 1996; Figure 1). This is supported by the predominant southward paleocurrent directions recently documented by Akdoğan et al. (2017) in the eastern and central parts of the Lower Cretaceous turbidites. Although the Early Cretaceous basin occupied a forearc position (Akdoğan et al., 2017) above the subduction zone (Aygül et al., 2015, 2016; Okay et al., 2006, 2013), the arc did not develop, probably due to flat subduction which is also reflected by the lack of Early Cretaceous zircons in the Lower Cretaceous turbidites (Akdoğan et al., 2017). The scarcity of the Early Cretaceous detrital zircons (<1%) in the Campanian-Maastrichtian sandstones provides further data for the absence of magmatism during Early Cretaceous subduction (Akdoğan et al., 2017; Aygül et al., 2015, 2016; Okay et al., 2006, 2013). In contrast, a broad arc magmatism took place in the Pontides during the Late Cretaceous leading to opening of the Black Sea basin as a back-arc basin (Görür, 1988; Okay & Nikishin, 2015; Tüysüz, 1999). With the opening of the Black Sea, the Ukrainian Shield was separated from the Pontides, and the Campanian-Maastrichtian forearc turbidites were sourced from the magmatic arc and from other local sources located in the southern margin of the Black Sea (Figures 12 and 13b). Paleoflows in the Campanian-Maastrichtian

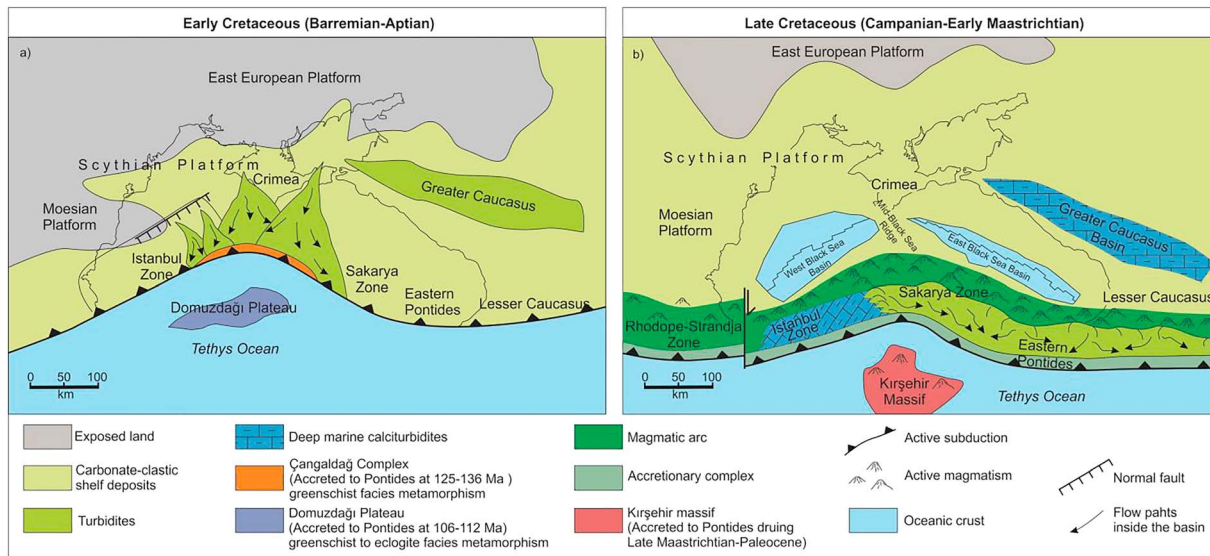


Figure 13. Paleotectonic environment of the Black Sea and surrounding regions and depositional areas of the Cretaceous turbidites. (a) Early Cretaceous (from Akdoğan et al., 2017) and (b) Late Cretaceous (this study).

turbidites are mainly axial with some northerly and easterly directions, indicating that the sediment dispersal was also different than those in the Lower Cretaceous turbidites (Figure 2 and Table S1). Such an abrupt change in the tectonic setting triggered by the opening of the Black Sea has influenced the source area and provides an example for the tectonic control on the sedimentation revealed by U–Pb detrital zircon ages.

6. Conclusion

Our new U–Pb detrital zircon ages, paleocurrent directions, and petrographic analysis from the Campanian–Maastrichtian turbidites and their comparison with those from the Lower Cretaceous turbidites of the eastern part of the central Pontides (Akdoğan et al., 2017; Okay et al., 2013) lead us the following conclusions:

- The Campanian–Maastrichtian turbidites were mainly sourced from the coeval Upper Cretaceous magmatic arc and from the basement rocks of the Pontides. On the contrary, the Lower Cretaceous turbidites were sourced mainly from the Archean–Paleoproterozoic basement rocks of the East European Platform (Akdoğan et al., 2017; Okay et al., 2013).
- The paleocurrent directions, the petrographic characteristics, and the detrital zircon age pattern of the Lower Cretaceous and Campanian–Maastrichtian turbidites of the eastern part of the central Pontides are different.
- The differences in the source areas of these two turbidite sequences are strictly controlled by the opening of the Black Sea, which cut off the sediment input from the East European Platform to the Pontides.

References

- Akdağ, K., & Kırmacı, M. Z. (2008). Submarine fan and slope-apron deposition in a Cretaceous forearc basin: The Gürsöğü formation (Kavak–Samsun, N. Turkey). *Journal of Asian Earth Sciences*, 31(4–6), 429–438. <https://doi.org/10.1016/j.jseas.2007.05.005>
- Akdoğan, R., Okay, A. I., Sunal, G., Tari, G., Meinhold, G., & Kylander-Clark, A. R. (2017). Provenance of a large Lower Cretaceous turbidite submarine fan complex on the active Laurasian margin: central Pontides, northern Turkey. *Journal of Asian Earth Sciences*, 134, 309–329. <https://doi.org/10.1016/j.jseas.2016.11.028>
- Allmendinger, R. W., Cardozo, N., & Fisher, D. M. (2011). *Structural Geology Algorithms: Vectors and Tensors*. Cambridge University Press. <https://doi.org/10.1017/CBO9780511920202>
- Aydın, M., Sahintürk, Ö., Serdar, H. S., Özçelik, I., Akarsu, I., Üngör, A., et al. (1986). Ballıdağ-Çangalıdağ (Kastamonu) arasındaki bölgenin jeolojisi. *Turkey Geological Survey Bulletin*, 29.
- Aydınçakır, E. (2016). Subduction-related Late Cretaceous high-K volcanism in the central Pontides orogenic belt: Constraints on geodynamic implications. *Geodinamica Acta*, 28(4), 379–411. <https://doi.org/10.1080/09853111.2016.1208526>
- Aygül, M., Okay, A. I., Oberhänsli, R., & Sudo, M. (2016). Pre-collisional accretionary growth of the southern Laurasian active margin, central Pontides, Turkey. *Tectonophysics*, 671, 218–234. <https://doi.org/10.1016/j.tecto.2016.01.010>

Acknowledgments

This study was supported by TÜBİTAK grants (2214-A) 109Y049 and 103R007 and TÜBA. We would like to thank Demir Altın for the paleontological determinations. Helps of Muhammed Ali Kuru during our field work of Nurullah Kızılay during mineral separation and of Andreas Kronz (Göttingen) during cathodoluminescence imaging are gratefully acknowledged. Finally, we are grateful to Editor Taylor Schildgen, Associate Editor Federico Rossetti, as well as reviewers William Cavazza Timur Ustaömer, and an anonymous reviewer for the constructive revisions which helped to clarify an earlier version of this manuscript. Additional data are available in the supporting information.

- Aygül, M., Okay, A. I., Oberhänsli, R., & Ziemann, M. A. (2015). Thermal structure of low-grade accreted Lower Cretaceous distal turbidites, the central Pontides, Turkey: Insights for tectonic thickening of an accretionary wedge. *Turkish Journal of Earth Sciences*, 24(5), 461–474. <https://doi.org/10.3906/yer-1504-4>
- Ballato, P., Parra, M., Schildgen, T. F., Dunkl, I., Yıldırım, C., Özsayın, E., et al. (2018). Multiple exhumation phases in the central Pontides (N Turkey): New temporal constraints on major geodynamic changes associated with the closure of the Neo-Tethys Ocean. *Tectonics*, 37(6), 1831–1857. <https://doi.org/10.1029/2017TC004808>
- Bibikova, E. V., Bogdanova, S. V., Larionov, A. N., Fedotova, A. A., Postnikov, A. V., Popova, L. P., et al. (2008). New data on the early Archean age of granitoids in the Volga-Ural segment of the East European Craton. *Doklady Earth Sciences*, 419(1), 243–247. SeP MAIK Nauka/Interperiodica. <https://doi.org/10.1134/S1028334X08020128>
- Bibikova, E. V., Bogdanova, S. V., Postnikov, A. V., Fedotova, A. A., Claesson, S., Kirnozova, T. I., et al. (2015). The early crust of the Volgo-Uralian segment of the East European Craton: Isotope-geochronological zirconology of metasedimentary rocks of the Bolshecheremshanskaya formation and their Sm-Nd model ages. *Stratigraphy and Geological Correlation*, 23(1), 1–23. <https://doi.org/10.1134/S0869593815010037>
- Bogdanova, S. V., Bingen, B., Gorbatshev, R., Kheraskova, T. N., Kozlov, V. I., Puchkov, V. N., & Volozh, Y. A. (2008). The East European Craton (Baltica) before and during the assembly of Rodinia. *Precambrian Research*, 160(1–2), 23–45. <https://doi.org/10.1016/j.precamres.2007.04.024>
- Bogdanova, S. V., De Waele, B., Bibikova, E. V., Belousova, E. A., Postnikov, A. V., Fedotova, A. A., & Lubov'P, P. (2010). Volgo-Uralia: The first U-Pb, Lu-Hf and Sm-Nd isotopic evidence of preserved Paleoproterozoic crust. *American Journal of Science*, 310(10), 1345–1383. <https://doi.org/10.2475/10.2010.06>
- Bracciali, L., Parrish, R. R., Najman, Y., Smye, A., Carter, A., & Wijbrans, J. R. (2016). Plio-Pleistocene exhumation of the eastern Himalayan syntaxis and its domal “pop-up”. *Earth-Science Reviews*, 160, 350–385. <https://doi.org/10.1016/j.earscirev.2016.07.010>
- Bussien, D., Gombojav, N., Winkler, W., & Von Quadt, A. (2011). The Mongol–Okhotsk Belt in Mongolia—An appraisal of the geodynamic development by the study of sandstone provenance and detrital zircons. *Tectonophysics*, 510(1–2), 132–150. <https://doi.org/10.1016/j.tecto.2011.06.024>
- Carrigan, C. W., Mukasa, S. B., Haydoutov, I., & Kolcheva, K. (2005). Age of Variscan magmatism from the Balkan sector of the orogen, central Bulgaria. *Lithos*, 82(1–2), 125–147. <https://doi.org/10.1016/j.lithos.2004.12.010>
- Cavazza, W., Federici, I., Okay, A. I., & Zattin, M. (2012). Apatite fission-track thermochronology of the western Pontides (NW Turkey). *Geological Magazine*, 149(01), 133–140. <https://doi.org/10.1017/S0016756811000525>
- Cawood, P. A., Nemchin, A. A., Strachan, R., Prave, T., & Krabbendam, M. (2007). Sedimentary basin and detrital zircon record along East Laurentia and Baltica during assembly and breakup of Rodinia. *Journal of the Geological Society*, 164(2), 257–275. <https://doi.org/10.1144/0016-76492006-115>
- Chen, F., Siebel, W., Satir, M., Terzioğlu, M., & Saka, K. (2002). Geochronology of the Karadere basement (NW Turkey) and implications for the geological evolution of the Istanbul zone. *International Journal of Earth Sciences*, 91(3), 469–481. <https://doi.org/10.1007/s00531-001-0239-6>
- Claesson, S., Bibikova, E., Bogdanova, S., & Skobelev, V. (2006). Archean terranes, Palaeoproterozoic reworking and accretion in the Ukrainian shield, East European Craton. *Geological Society, London, Memoirs*, 32(1), 645–654. <https://doi.org/10.1144/GSL.MEM.2006.32.01.38>
- Corfu, F. (2003). Atlas of zircon textures. *Reviews in Mineralogy & Geochemistry*, 53(1), 469–500. <https://doi.org/10.2113/0530469>
- Critelli, S., & Ingersoll, R. V. (1995). Interpretation of neovolcanic versus palaeovolcanic sand grains: An example from Miocene deep-marine sandstone of the Topanga Group (Southern California). *Sedimentology*, 42(5), 783–804. <https://doi.org/10.1111/j.1365-3091.1995.tb00409.x>
- DeGraaff-Surpless, K., Graham, S. A., Wooden, J. L., & McWilliams, M. O. (2002). Detrital zircon provenance analysis of the Great Valley Group, California: Evolution of an arc-forearc system. *Geological Society of America Bulletin*, 114(12), 1564–1580. [https://doi.org/10.1130/0016-7606\(2002\)114<1564:DZPAOT>2.0.CO;2](https://doi.org/10.1130/0016-7606(2002)114<1564:DZPAOT>2.0.CO;2)
- Delibaş, O., Moritz, R., Ulianov, A., Chiaradia, M., Saraç, C., Revan, K. M., & Göç, D. (2016). Cretaceous subduction-related magmatism and associated porphyry-type Cu–Mo prospects in the eastern Pontides, Turkey: New constraints from geochronology and geochemistry. *Lithos*, 248, 119–137.
- Dickinson, W. R. (1970). Interpreting detrital modes of graywacke and arkose. *Journal of Sedimentary Research*, 40(2), 695–707.
- Dickinson, W. R. (1995). Forearc basins. In C. J. Busby & R. V. Ingersoll (Eds.), *Tectonics of Sedimentary Basins* (pp. 221–261). Cambridge: Blackwell Science.
- Dickinson, W. R., Beard, L. S., Brakenridge, G. R., Erjavec, J. L., Ferguson, R. C., Inman, K. F., et al. (1983). Provenance of North American Phanerozoic sandstones in relation to tectonic setting. *Geological Society of America Bulletin*, 94(2), 222–235. [https://doi.org/10.1130/0016-7606\(1983\)94<222:PONAPS>2.0.CO;2](https://doi.org/10.1130/0016-7606(1983)94<222:PONAPS>2.0.CO;2)
- Dokuz, A. (2011). A slab detachment and delamination model for the generation of carboniferous high potassium I-type magmatism in the eastern Pontides, NE Turkey: Köse composite pluton. *Gondwana Research*, 19(4), 926–944. <https://doi.org/10.1016/j.gr.2010.09.006>
- Dong, Y., Liu, X., Neubauer, F., Zhang, G., Tao, N., Zhang, Y., et al. (2013). Timing of Paleozoic amalgamation between the North China and South China blocks: Evidence from detrital zircon U–Pb ages. *Tectonophysics*, 586, 173–191. <https://doi.org/10.1016/j.tecto.2012.11.018>
- Ellero, A., Ottria, G., Sayit, K., Catanzariti, R., Frassi, C., Göncüoğlu, M. C., et al. (2015). Geological and geochemical evidence for a Late Cretaceous continental arc in the central Pontides, northern Turkey. *Ofioliti*, 40(2), 73–90.
- Espurt, N., Hippolyte, J. C., Kaymakci, N., & Sangu, E. (2014). Lithospheric structural control on inversion of the southern margin of the Black Sea Basin, Central Pontides, Turkey. *Lithosphere*, 6(1), 26–34.
- Eyüboğlu, Y. (2015). Petrogenesis and U–Pb zircon chronology of felsic tuffs interbedded with turbidites (eastern Pontides Orogenic Belt, NE Turkey): Implications for Mesozoic geodynamic evolution of the eastern Mediterranean region and accumulation rates of turbidite sequences. *Lithos*, 212, 74–92.
- Fedo, C. M., Sircombe, K. N., & Rainbird, R. H. (2003). Detrital zircon analysis of the sedimentary record. *Reviews in Mineralogy & Geochemistry*, 53(1), 277–303. <https://doi.org/10.2113/0530277>
- Folk, R. L., Andrews, P. B., & Lewis, D. (1970). Detrital sedimentary rock classification and nomenclature for use in New Zealand. *New Zealand Journal of Geology and Geophysics*, 13(4), 937–968. <https://doi.org/10.1080/00288306.1970.10418211>
- Frassi, C., Marroni, M., Pandolfi, L., Göncüoğlu, M. C., Ellero, A., Ottria, G., et al. (2018). Burial and exhumation history of the Daday unit (central Pontides, Turkey): Implications for the closure of the intra-Pontide oceanic basin. *Geological Magazine*, 155(2), 356–376.

- Gazzi, P. (1966). Le arenarie del flysch sopracretaceo dell'Appennino modenese; Correlazioni con flysch di Monghidoro. *Miner Petrogr Acta*, 12, 69–97.
- Gedik, A., & Korkmaz, S. (1984). Sinop havzasının jeolojisi ve petrol olanakları. *Geological Engineering*, 19, 53–79. (in Turkish with English abstract)
- Gehrels, G. (2014). Detrital zircon U-Pb geochronology applied to tectonics. *Annual Review of Earth and Planetary Sciences*, 42(1), 127–149. <https://doi.org/10.1146/annurev-earth-050212-124012>
- Gehrels, G. E., & Dickinson, W. R. (1995). Detrital zircon provenance of Cambrian to Triassic miogeoclinal and eugeoclinal strata in Nevada. *American Journal of Science*, 295(1), 18–48. <https://doi.org/10.2475/ajs.295.1.18>
- Görür, N. (1988). Timing of opening of the Black Sea basin. *Tectonophysics*, 147(3–4), 247–262. [https://doi.org/10.1016/0040-1951\(88\)90189-8](https://doi.org/10.1016/0040-1951(88)90189-8)
- Görür, N., Tüysüz, O., Aykol, A., Sakıncı, M., Yiğitbaş, E., & Akkök, R. (1993). Cretaceous red pelagic carbonates of northern Turkey—Their place in the opening history of the Black-Sea. *Eclogae Geologicae Helveticae*, 86, 819–838.
- Gradstein, F. M., Ogg, J. G., Schmitz, M. D., & Ogg, G. M. (2012). *The Geologic Time Scale 2012*. Boston, MA: Elsevier.
- Güçer, M. A., Arslan, M., Sherlock, S., & Heaman, L. M. (2016). Permo-Carboniferous granitoids with Jurassic high temperature metamorphism in central Pontides, northern Turkey. *Mineralogy and Petrology*, 110(6), 943–964. <https://doi.org/10.1007/s00710-016-0443-5>
- Hakymez, H. Y., & Papak, I. (2002). Geological map of Turkey, Samsun, (Scale 1:500,000), Maden Tetkik ve Arama Müdürlüğü (MTA), Ankara.
- Hippolyte, J. C., Espurt, N., Kaymakci, N., Sangu, E., & Müller, C. (2016). Cross-sectional anatomy and geodynamic evolution of the central Pontide orogenic belt (northern Turkey). *International Journal of Earth Sciences*, 105(1), 81–106. <https://doi.org/10.1007/s00531-015-1170-6>
- Hippolyte, J. C., Müller, C., Kaymakci, N., & Sangu, E. (2010). Dating of the Black Sea Basin: New nannoplankton ages from its inverted margin in the central Pontides (Turkey). *Geological Society, London, Special Publications*, 340(1), 113–136. <https://doi.org/10.1144/SP340.7>
- Hoskin, P. W. O., & Schaltegger, U. (2003). The composition of zircon and igneous and metamorphic petrogenesis. *Reviews in Mineralogy and Geochemistry*, 53(1), 27–62. <https://doi.org/10.2113/0530027>
- Ingersoll, R. V. (2012). Tectonics of sedimentary basins, with revised nomenclature. In C. Busby & A. Azor (Eds.), *Tectonics of Sedimentary Basins: Recent Advances* (pp. 1–43). Chichester, UK: John Wiley.
- Karsli, O., Caran, Ş., Dokuz, A., Çoban, H., Chen, B., & Kandemir, R. (2012). A-type granitoids from the eastern Pontides, NE Turkey: Records for generation of hybrid A-type rocks in a subduction-related environment. *Tectonophysics*, 530, 208–224.
- Karsli, O., Dokuz, A., Uysal, I., Aydın, F., Chen, B., Kandemir, R., & Wijbrans, J. (2010). Relative contributions of crust and mantle to generation of Campanian high-K calc-alkaline I-type granitoids in a subduction setting, with special reference to the Harşit Pluton, eastern Turkey. *Contributions to Mineralogy and Petrology*, 160(4), 467–487. <https://doi.org/10.1007/s00410-010-0489-z>
- Karshoğlu, Ö., Ustaömer, T., Robertson, A. H. F., & Peytcheva, I. (2012). Age and provenance of detrital zircons from a sandstone turbidite of the Triassic-early Jurassic Küre complex, central Pontides. In Abstracts, *International Earth Science Colloquium on the Aegean Region*, IAESCA (p. 57).
- Kaygusuz, A., Arslan, M., Siebel, W., Sipahi, F., İlbeyli, N., & Temizel, İ. (2014). LA-ICP MS zircon dating, whole-rock and Sr-Nd-Pb-O isotope geochemistry of the Camiboğazi pluton, eastern Pontides, NE Turkey: Implications for lithospheric mantle and lower crustal sources in arc-related I-type magmatism. *Lithos*, 192, 271–290.
- Kaygusuz, A., & Şen, C. (2011). Calc-alkaline I-type plutons in the eastern Pontides, NE Turkey: U-Pb zircon ages, geochemical and Sr-Nd isotopic compositions. *Chemie der Erde-Geochemistry*, 71(1), 59–75. <https://doi.org/10.1016/j.chemer.2010.07.005>
- Kaygusuz, A., Siebel, W., Şen, C., & Satir, M. (2008). Petrochemistry and petrology of I-type granitoids in an arc setting: The composite Torul pluton, eastern Pontides, NE Turkey. *International Journal of Earth Sciences*, 97(4), 739–764. <https://doi.org/10.1007/s00531-007-0188-9>
- Keskin, M., & Tüysüz, O. (2018). Stratigraphy, petrogenesis and geodynamic setting of Late Cretaceous volcanism on the SW margin of the Black Sea, Turkey. *Geological Society, London, Special Publications*, 464, SP464–SP465.
- Kortyna, C., Donaghy, E., Trop, J. M., & Idleman, B. (2014). Integrated provenance record of a forearc basin modified by slab-window magmatism: Detrital-zircon geochronology and sandstone compositions of the Paleogene Arkose Ridge formation, south-Central Alaska. *Basin Research*, 26(3), 436–460. <https://doi.org/10.1111/bre.12033>
- Leren, B. L. (2003). Late Cretaceous to Early Eocene sedimentation in the Sinop-Boyabat Basin, north-central Turkey: Facies analysis of turbiditic to shallow-marine deposits. (Master's thesis). The University of Bergen. Retrieved from Bergen Open Research Archive (BORA).
- Leren, B. L., Janbu, N. E., Nemec, W., Kirman, E., & İlgar, A. (2007). Late Cretaceous to Early Eocene sedimentation in the Sinop-Boyabat Basin, north-central Turkey: A deep-water turbiditic system evolving into littoral carbonate platform. In *Sedimentary Processes, Environments and Basins* (pp. 401–456). <https://doi.org/10.1002/9781444304411.ch18>
- Marroni, M., Frassi, C., Gönçüoğlu, M. C., Di Vincenzo, G., Pandolfi, L., Rebay, G., et al. (2014). Late Jurassic amphibolite-facies metamorphism in the Intra-Pontide Suture Zone (Turkey): An eastward extension of the Vardar Ocean from the Balkans into Anatolia? *Journal of the Geological Society London*, 171(5), 605–608. <https://doi.org/10.1144/jgs2013-104>
- Mayringer, F., Treloar, P. J., Gerdes, A., Finger, F., & Shengelia, D. (2011). New age data from the Dzirula massif, Georgia: Implications for the evolution of the Caucasian Variscides. *American Journal of Science*, 311(5), 404–441. <https://doi.org/10.2475/05.2011.02>
- Meijers, M. J., Kaymakci, N., Van Hinsbergen, D. J., Langereis, C. G., Stephenson, R. A., & Hippolyte, J. C. (2010). Late Cretaceous to Paleocene oroclinal bending in the central Pontides (Turkey). *Tectonics*, 29, TC4016. <https://doi.org/10.1029/2009TC002620>
- Moore, W. J., McKee, E. H., & Ye Akinçi, Ö. (1980). *Chemistry and Chronology of Plutonic Rocks in the Pontide Mountains, Northern Turkey* (pp. 209–216). Belgrade, Yugoslavia: Symposium on the European copper deposits.
- Nikishin, A. M., Okay, A. I., Tüysüz, O., Demirel, A., Amelin, N., & Petrov, E. (2015). The Black Sea basins structure and history: New model based on new deep penetration regional seismic data. Part 1: Basins structure and fill. *Marine and Petroleum Geology*, 59, 638–655. <https://doi.org/10.1016/j.marpetgeo.2014.08.017>
- Nzege, O. M. (2008). *Petrogenesis and Geochronology of the Deliktaş, Sivrikaya and Devrekani Granitoids and Basement, Kastamonu Belt-Central Pontides (NW Turkey): Evidence for Late Palaeozoic-Mesozoic Plutonism, and Geodynamic Interpretation*, Ddoctoral dissertation. Germany: University of Tübingen. <http://citeseerx.ist.psu.edu/viewdoc/download?doi=10.1.1.1004.9672&rep=rep1&type=pdf>
- Nzege, O. M., Satir, M., Siebel, W., & Taubald, H. (2006). Geochemical and isotopic constraints on the genesis of the Late Palaeozoic Deliktaş and Sivrikaya granites from the Kastamonu granitoid belt (central Pontides, Turkey). *Neues Jahrbuch für Mineralogie-Abhandlungen*, 183(1), 27–40.

- Ohta, E., Dogan, R., Batic, H., & Abe, M. (1988). Geology and mineralization of Dereköy porphyry copper deposits, northern Thrace, Turkey. *Bulletin of the Geological Survey of Japan*, 39(2), 115–134.
- Okay, A. I., Altın, D., Sunal, G., Aygöl, M., Akdoğan, R., & Altın, S. ve Simmons, M. (2018). Geological evolution of the central Pontides. *Geological Society, London, Special Publications*, 464, SP464–SP463. <https://doi.org/10.1144/SP464.3>
- Okay, A. I., & Nikishin, A. M. (2015). Tectonic evolution of the southern margin of Laurasia in the Black Sea region. *International Geology Review*, 57(5–8), 1051–1076. <https://doi.org/10.1080/00206814.2015.1010609>
- Okay, A. I., & Şahintürk, Ö. (1997). Geology of the eastern Pontides. In A. G. Robinson (Ed.), *Regional and Petroleum Geology of the Black Sea and Surrounding Region* (Vol. 68, pp. 291–311). Tulsa, Oklahoma: American Association of Petroleum Geologists Memoir.
- Okay, A. I., Satır, M., Tüysüz, O., Akyüz, S., & Chen, F. (2001). The tectonics of the Strandja Massif: Variscan and mid-Mesozoic deformation and metamorphism in the northern Aegean. *International Journal of Earth Sciences*, 90(2), 217–233. <https://doi.org/10.1007/s005310000104>
- Okay, A. I., Sunal, G., Sherlock, S., Altın, D., Tüysüz, O., Kylander-Clark, A. R., & Aygöl, M. (2013). Early Cretaceous sedimentation and orogeny on the active margin of Eurasia: Southern central Pontides, Turkey. *Tectonics*, 32, 1247–1271. <https://doi.org/10.1002/tect.20077>
- Okay, A. I., Sunal, G., Tüysüz, O., Sherlock, S., Keskin, M., & Kylander-Clark, A. R. C. (2014). Low-pressure–high-temperature metamorphism during extension in a Jurassic magmatic arc, central Pontides, Turkey. *Journal of Metamorphic Geology*, 32(1), 49–69. <https://doi.org/10.1111/jmg.12058>
- Okay, A. I., & Tüysüz, O. (1999). Tethyan sutures of northern Turkey. *Geological Society of London, Special Publication*, 156(1), 475–515. <https://doi.org/10.1144/GSL.SP.1999.156.01.22>
- Okay, A. I., Tuysuz, O., Satır, M., Ozkan-Altın, S., Altın, D., Sherlock, S., & Eren, R. H. (2006). Cretaceous and Triassic subduction-accretion, high-pressure–low-temperature metamorphism, and continental growth in the central Pontides, Turkey. *Geological Society of America Bulletin*, 118(9–10), 1247–1269. <https://doi.org/10.1130/B25938.1>
- Okay, N., Zack, T., Okay, A. I., & Barth, M. (2011). Sinistral transport along the trans-European suture zone: Detrital zircon–rutile geochronology and sandstone petrography from the Carboniferous flysch of the Pontides. *Geological Magazine*, 148(03), 380–403. <https://doi.org/10.1017/S0016756810000804>
- Orme, D. A., Carrapa, B., & Kapp, P. (2015). Sedimentology, provenance and geochronology of the Upper Cretaceous–Lower Eocene western Xigaze forearc basin, southern Tibet. *Basin Research*, 27(4), 387–411. <https://doi.org/10.1111/bre.12080>
- Özcan, E., & Özkan-Altın, S. (1999). The genera *Lepidobitoides* and *Orbitoides*: Evolution and stratigraphic significance in some Anatolian basins. *Geological Journal*, 34(3), 275–286. [https://doi.org/10.1002/\(SICI\)1099-1034\(199907/09\)34:3<275::AID-GJ827>3.0.CO;2-J](https://doi.org/10.1002/(SICI)1099-1034(199907/09)34:3<275::AID-GJ827>3.0.CO;2-J)
- Özcan, Z., Okay, A. I., Özcan, E., Hakyemez, A., & Altın, S. Ö. (2012). Late Cretaceous–Eocene geological evolution of the Pontides based on new stratigraphic and paleontologic data between the Black Sea coast and Bursa (NW Turkey). *Turkish Journal of Earth Sciences*, 21, 933–960.
- Özdamar, Ş. (2016). Geochemistry and geochronology of late Mesozoic volcanic rocks in the northern part of the eastern Pontide Orogenic Belt (NE Turkey): Implications for the closure of the Neo-Tethys Ocean. *Lithos*, 248, 240–256.
- Özgül, N. (2012). Stratigraphy and some structural features of the Istanbul Palaeozoic. *Turkish Journal of Earth Science*, 21, 817–866.
- Özkan-Altın, S., & Özcan, E. (1999). Upper Cretaceous planktonic foraminiferal biostratigraphy from NW Turkey: Calibration of the stratigraphic ranges of larger benthonic foraminifera. *Geological Journal*, 34(3), 287–301. [https://doi.org/10.1002/\(SICI\)1099-1034\(199907/09\)34:3<287::AID-GJ828>3.0.CO;2-B](https://doi.org/10.1002/(SICI)1099-1034(199907/09)34:3<287::AID-GJ828>3.0.CO;2-B)
- Rubatto, D. (2002). Zircon trace element geochemistry: Partitioning with garnet and the link between U–Pb ages and metamorphism. *Chemical Geology*, 184(1–2), 123–138. [https://doi.org/10.1016/S0009-2541\(01\)00355-2](https://doi.org/10.1016/S0009-2541(01)00355-2)
- Sharman, G. R., Graham, S. A., Grove, M., Kimbrough, D. L., & Wright, J. E. (2015). Detrital zircon provenance of the Late Cretaceous–Eocene California forearc: Influence of Laramide low-angle subduction on sediment dispersal and paleogeography. *Geological Society of America Bulletin*, 127(1–2), 38–60. <https://doi.org/10.1130/B31065.1>
- Shchipansky, A. A., & Bogdanova, S. V. (1996). The Sarmatian crustal segment: Precambrian correlation between the Voronezh massif and the Ukrainian Shield across the Dniepr–Donets aulacogen. *Tectonophysics*, 268(1–4), 109–125. [https://doi.org/10.1016/S0040-1951\(96\)00227-2](https://doi.org/10.1016/S0040-1951(96)00227-2)
- Sunal, G. (2013). Devonian magmatism in the western Sakarya zone, Karacabey region, NW Turkey. *Geodinamica Acta*, 25, 183–201.
- Sunal, G., Natal'in, B. A., Satır, M., & Toraman, E. (2006). Paleozoic magmatic events in the Strandja Massif, NW Turkey. *Geodinamica Acta*, 19(5), 283–300. <https://doi.org/10.3166/ga.19.283-300>
- Sunal, G., Satır, M., Natal'in, B. A., & Toraman, E. (2008). Paleotectonic position of the Strandja Massif and surrounding continental blocks based on zircon Pb–Pb age studies. *International Geology Review*, 50(6), 519–545. <https://doi.org/10.2747/0020-6814.50.6.519>
- Topuz, G., Altherr, R., Schwarz, W. H., Dokuz, A., & Meyer, H. P. (2007). Variscan amphibolite-facies rocks from the Kurtuluş metamorphic complex (Gümüşhane area, eastern Pontides, Turkey). *International Journal of Earth Sciences*, 96(5), 861–873. <https://doi.org/10.1007/s00531-006-0138-y>
- Topuz, G., Altherr, R., Siebel, W., Schwarz, W. H., Zack, T., Hasözbe, A., et al. (2010). Carboniferous high-potassium I-type granitoid magmatism in the eastern Pontides: The Gümüşhane pluton (NE Turkey). *Lithos*, 116(1–2), 92–110. <https://doi.org/10.1016/j.lithos.2010.01.003>
- Tüysüz, O. (1999). Geology of the Cretaceous sedimentary basins of the Western Pontides. *Geological Journal*, 34(1–2), 75–93. [https://doi.org/10.1002/\(SICI\)1099-1034\(199901/06\)34:1/2<75::AID-GJ815>3.0.CO;2-S](https://doi.org/10.1002/(SICI)1099-1034(199901/06)34:1/2<75::AID-GJ815>3.0.CO;2-S)
- Tüysüz, O. (2018). Cretaceous geological evolution of the Pontides. *Geological Society, London, Special Publications*, 464, SP464–SP469. <https://doi.org/10.1144/SP464.9>
- Tüysüz, O., Melinte-Dobrinescu, M. C., Yılmaz, İ. Ö., Kirici, S., Švabenická, L., & Skupien, P. (2016). The Kapanboğazi formation: A key unit for understanding Late Cretaceous evolution of the Pontides, N Turkey. *Palaeogeography, Palaeoclimatology, Palaeoecology*, 441, 565–581. <https://doi.org/10.1016/j.palaeo.2015.06.028>
- Uğuz, M. F., Sevin, M., & Duru, M. (2002). Geological map of Turkey. 1: 500.000 scaled Sinop sheet, Maden Tetkik ve Arama Genel Müdürlüğü, Ankara.
- Ustaömer, P. A., Ustaömer, T., & Robertson, A. (2012). Ion probe U–Pb dating of the central Sakarya basement: A peri-Gondwana terrane intruded by late Lower Carboniferous subduction/collision-related granitic rocks. *Turkish Journal of Earth Sciences*, 21(6), 905–932.
- Ustaömer, T., Robertson, A. H., Ustaömer, P. A., Gerdes, A., & Peytcheva, I. (2013). Constraints on Variscan and Cimmerian magmatism and metamorphism in the Pontides (Yusufeli–Artvin area), NE Turkey from U–Pb dating and granite geochemistry. *Geological Society, London, Special Publications*, 372(1), 49–74. <https://doi.org/10.1144/SP372.13>
- Ustaömer, T., & Robertson, A. H. F. (1994). Late Palaeozoic marginal basin and subduction-accretion: The Palaeotethyan Küre complex, central Pontides, northern Turkey. *Journal of the Geological Society*, 151(2), 291–305. <https://doi.org/10.1144/gsjgs.151.2.0291>

- Ustaömer, T., Ustaömer, P. A., Robertson, A. H., & Gerdes, A. (2016). Implications of U–Pb and Lu–Hf isotopic analysis of detrital zircons for the depositional age, provenance and tectonic setting of the Permian–Triassic Palaeotethyan Karakaya complex, NW Turkey. *International Journal of Earth Sciences*, 105(1), 7–38. <https://doi.org/10.1007/s00531-015-1225-8>
- Yılmaz, O., & Boztuğ, D. (1986). Kastamonu granitoid belt of northern Turkey: First arc plutonism product related to the subduction of the paleo-Tethys. *Geology*, 14(2), 179–183. [https://doi.org/10.1130/0091-7613\(1986\)14<179:KGBONT>2.0.CO;2](https://doi.org/10.1130/0091-7613(1986)14<179:KGBONT>2.0.CO;2)
- Yılmaz-Şahin, S., Aysal, N., Güngör, Y., Peytcheva, I., & Neubauer, F. (2014). Geochemistry and U–Pb zircon geochronology of metagranites in Istranca (Strandja) Zone, NW Pontides, Turkey: Implications for the geodynamic evolution of Cadomian orogeny. *Gondwana Research*, 26(2), 755–771.
- Zuffa, G. G. (1985). Optical analyses of arenites: Influence of methodology on compositional results. In G. G. Zuffa (Ed.), *Provenance of Arenites* (pp. 165–189). NATO-ASI: Reidel Publ Co, Dordrecht. https://doi.org/10.1007/978-94-017-2809-6_8

References From the Supporting Information

- Dunkl, I., Mikes, T., Simon, K., & Von Eynatten, H. (2008). Brief introduction to the Windows program Pepita: Data visualization, and reduction, outlier rejection, calculation of trace element ratios and concentrations from LAICPMS data. *Mineralogical Association of Canada, Short Course*, 40, 334–340.
- Jackson, S. E., Pearson, N. J., Griffin, W. L., & Belousova, E. A. (2004). The application of laser ablation-inductively coupled plasma-mass spectrometry to in situ U–Pb zircon geochronology. *Chemical Geology*, 211(1–2), 47–69. <https://doi.org/10.1016/j.chemgeo.2004.06.017>
- Ludwig, K. R. (2012). User's manual for Isoplot 3.75: A geochronological toolkit for Microsoft Excel. *Berkeley Geochronology Center Special Publication*, No. 5, 75 p.
- Paces, J. B., & Miller, J. D. (1993). Precise U–Pb ages of Duluth complex and related mafic intrusions, northeastern Minnesota: Geochronological insights to physical, petrogenetic, paleomagnetic, and tectonomagmatic processes associated with the 1.1 Ga mid-continent rift system. *Journal of Geophysical Research*, 98, 13997–14013. <https://doi.org/10.1029/93JB01159>
- Sircombe, K. N. (2004). AgeDisplay: An EXCEL workbook to evaluate and display univariate geochronological data using binned frequency histograms and probability density distributions. *Computers & Geosciences*, 30(1), 21–31. <https://doi.org/10.1016/j.cageo.2003.09.006>
- Sláma, J., Košler, J., Condon, D. J., Crowley, J. L., Gerdes, A., Hanchar, J. M., et al. (2008). Plešovice zircon—A new natural reference material for U–Pb and Hf isotopic microanalysis. *Chemical Geology*, 249(1–2), 1–35. <https://doi.org/10.1016/j.chemgeo.2007.11.005>
- Wiedenbeck, W., Alle, P., Corfu, F., Griffin, W. L., Meier, M., Oberli, F. V., et al. (1995). Three natural zircon standards for U–Th–Pb, Lu–Hf, trace element and REE analyses. *Geostandards and Geoanalytical Research*, 19(1), 1–23. <https://doi.org/10.1111/j.1751-908X.1995.tb00147.x>